Discovery of pyrazolo-thieno[3,2-d]pyrimidinylamino-phenyl acetamides as type-II pan-tropomyosin receptor kinase (TRK) inhibitors: Design, synthesis, and biological evaluation

Wei Yan, Lingtian Zhang, Fengping Lv, Marialuisa Moccia, Francesca Carlomagno, Christophe Landry, Massimo Santoro, Fabien Gosselet, Brendan Frett, Hong-Yu Li

European Journal of Medicinal Chemistry

Discovery of pyrozolo-thienopyrimidinylamino-phenyl acetamides as type-II pan-tropomyosin receptor kinase (TRK) inhibitors: design, synthesis, and biological evaluation

--Manuscript Draft--

Manuscript Number:	EJMECH-D-20-02632R1
Article Type:	Full Paper
Keywords:	kinase inhibitor, TRKA, type-II, colorectal cancer
Corresponding Author:	Hong-yu Li, Ph.D College of Pharmacy, University of Arizona Tucson, AZ United States
First Author:	Wei Yan
Order of Authors:	Wei Yan
	Lingtian Zhang
	Fengping Lv
	Marialuisa Moccia
	francesca carlomagno
	Christophe Landry
	Massimo Santoro
	Fabien Gosselet
	Brendan Frett
	Hong-yu Li, Ph.D
Abstract:	Tropomyosin receptor kinase (TRK) represents an attractive oncology target for cancer therapy related to its critical role in cancer formation and progression. NTRK fusions are found to occur in 3.3% of lung cancers, 2.2% of colorectal cancers, 16.7% of thyroid cancers, 2.5% of glioblastomas, and 7.1% of pediatric gliomas. In this paper, we described the discovery of the type-II pan-TRK inhibitor 4c through the structure-based drug design strategy from the original hits 1b and 2b . Compound 4c exhibited excellent in vitro TRKA, TRKB, and TRKC kinase inhibitory activity and anti-proliferative activity against human colorectal carcinoma derived cell line KM12. In the NCI-60 human cancer cell lines screen, compound 4g demonstrated nearly 80% of growth inhibition for KM12, while only minimal inhibitory activity was observed for the remaining 59 cancer cell lines. Western blot analysis demonstrated that 4c and its urea cousin 4k suppressed the TPM3-TRKA autophosphorylation at the concentrations of 100 nM and 10 nM, respectively. The work presented that 2-(4-(thieno[3,2- d]pyrimidin-4-ylamino)phenyl)acetamides could serve as a novel scaffold for the discovery and development of type-II pan-TRK inhibitors for the treatment of TRK driven cancers.
Suggested Reviewers:	Sarah Skerratt sarahskerratt1@gmail.com Expert in the field
	Nicholas Mcconnell Nicholas.Mcconnell@ucsf.edu Expert in the field.

Graphical abstract:

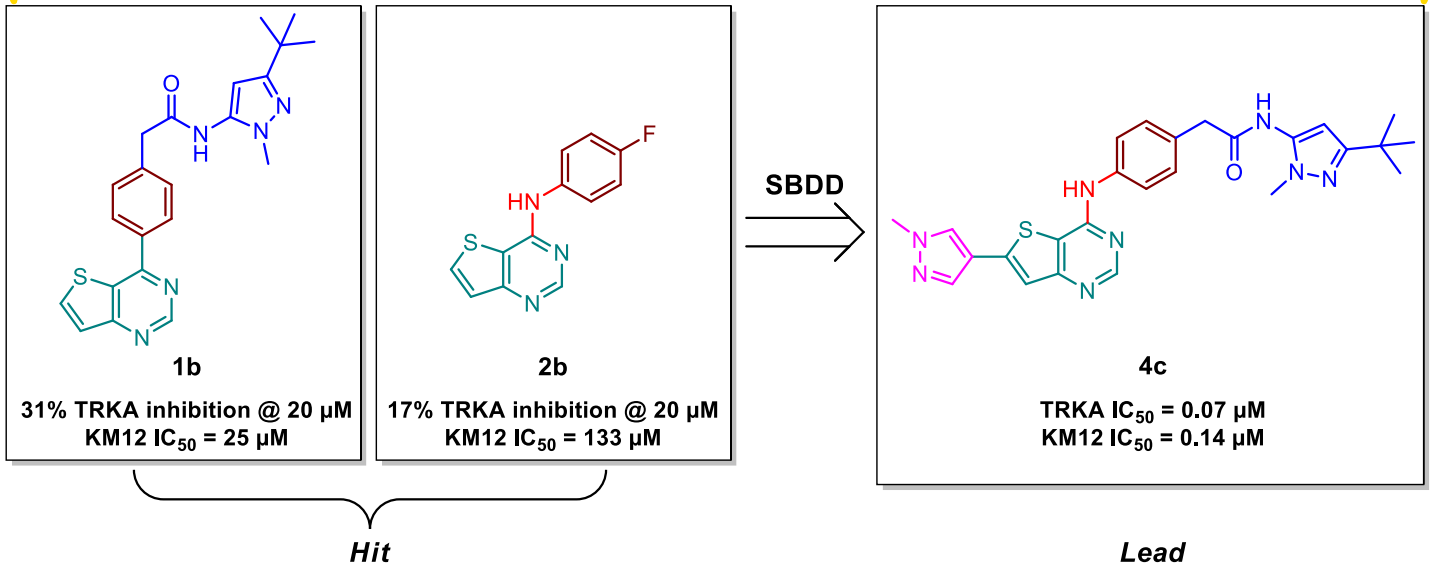

PDF-XChange Editor Click to BUY NOW! www.tracker-software.com

Highlights:

- A series of novel thieno[3,2-*d*]pyrimidine type-II TRKA inhibitors were designed and synthesized.
- Representative compound **4c** was discovered through structure-based drug design (SBDD) approach
- Compound **4c** showed potent *in vitro* anti-proliferative activity.
- Compound **4c** exhibited an effective blockage of TRKA autophosphorylation.

Discovery of pyrozolo-thienopyrimidinylamino-phenyl acetamides as type-II pan-tropomyosin receptor kinase (TRK) inhibitors: design, synthesis, and biological evaluation

Wei Yan,[1,†] Lingtian Zhang,[1,†] Fengping Lv,[1] Marialuisa Moccia,[2] Francesca Carlomagno,[2,3] Christophe Landry,[4] Massimo Santoro,[2] Fabien Gosselet,[4] Brendan Frett,[1] and Hong-yu Li[1,*]

[1]Department of Pharmaceutical Sciences, College of Pharmacy, University of Arkansas for Medical Sciences, Little Rock, AR 72205, USA

[2]Dipartimento di Medicina Molecolare e Biotecnologie Mediche, Università Federico II, Via S Pansini 5, 80131 Naples, Italy

[3]Istituto di Endocrinologia e Oncologia Sperimentale del CNR, Via S Pansini 5, 80131 Naples, Italy

[4]Blood Brain Barrier Laboratory (LBHE), University of Artois, UR2465, F-62300, Lens, France

Abstract

Tropomyosin receptor kinase (TRK) represents an attractive oncology target for cancer therapy related to its critical role in cancer formation and progression. *NTRK* fusions are found to occur in 3.3% of lung cancers, 2.2% of colorectal cancers, 16.7% of thyroid cancers, 2.5% of glioblastomas, and 7.1% of pediatric gliomas. In this paper, we described the discovery of the type-II pan-TRK inhibitor **4c** through the structure-based drug design strategy from the original hits **1b** and **2b**. Compound **4c** exhibited excellent *in vitro* TRKA, TRKB, and TRKC kinase inhibitory activity and anti-proliferative activity against human colorectal carcinoma derived cell line KM12. In the NCI-60 human cancer cell lines screen, compound **4g** demonstrated nearly 80% of growth inhibition for KM12, while only minimal inhibitory activity was observed for the remaining 59 cancer cell lines. Western blot analysis demonstrated that **4c** and its urea cousin **4k** suppressed the TPM3-TRKA autophosphorylation at the concentrations of 100 nM and 10 nM, respectively. The work presented that 2-(4-(thieno[3,2-*d*]pyrimidin-4-

ylam[illegible])phenyl)acetamides could serve as a novel scaffold for the discovery and development of type-II pan-TRK inhibitors for the treatment of TRK driven cancers.

Keywords: kinase inhibitor, TRK, type-II, colorectal cancer

Introduction

The tropomyosin receptor kinase (TRK) family enzymes belong to the transmembrane receptor tyrosine kinases superfamily. The TRKs are primarily expressed in human neuronal tissues that regulate synaptic strength and plasticity in the mammalian nervous system.[1-2] The TRK family consists of three subtypes, and each is activated by a specific ligand: TRKA and TRKB are activated by nerve growth factor (NGF) and brain-derived neurotrophic factor (BDNF), respectively, while TRKC is primarily turned on by neurotrophin 3 (NT3).[1-3] Upon ligand binding, TRKs become dimerized and autophosphorylated thus trigger downstream signal transduction pathways including RAS/mitogen-activated protein kinase (MAPK), phosphatidylinositol 3 kinase (PI3K)/protein kinase B (AKT), and phospholipase C-γ (PLC-γ)/PKC pathways, which consequently modulate cell growth, proliferation, survival, and differentiation.[4] Initially, the TRKA oncogene was discovered in colon cancer.[5-6] So far, *NTRK* fusions are found to occur in 3.3% of lung cancers, 2.2% of colorectal cancers, 16.7% of thyroid cancers, 2.5% of glioblastomas, and 7.1% of pediatric gliomas.[3] Within the TRK family, TRKA is the most commonly identified oncogene, which is found at a rate of approximately 7.4% across multiple tumor types (0.4% for TRKB and 3.4% for TRKA, respectively).[3, 7] Moreover, it has been found that TRKA also mediates the stimulation of early tumor progression.[8] Therefore, the blockade of TRKA signaling is considered as an attractive clinical approach for the treatment of cancers.

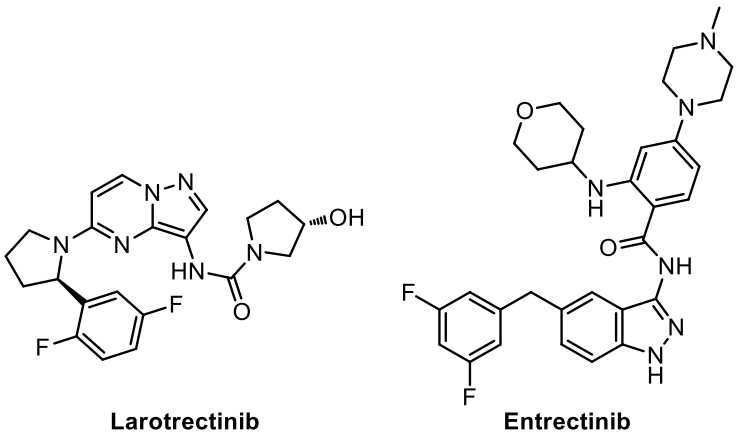

Figure 1. Chemical structures of larotrectinib (Vitrakvi®) and entrectinib (Rozlytrek®).

To date, only two TRKA inhibitors were approved by U.S. food and drug administration. Larotrectinib was approved in November 2018 for solid tumors with *NTRK* gene fusions;[9] and entrectinib was approved in August 2019 for *NTRK* gene fusion-positive solid tumors or ROS1-positive non-small cell lung cancer.[10] According to the classification of Shokat *et al.*, [11] these two drugs both belong to type-I kinase inhibitor. Type-I inhibitors bind to the kinase only at the highly conserved adenosine triphosphate (ATP) binding site in the "DFG-motif in" (active) conformation and are thus less selective or active. Distinct from type-I inhibitors, type-II inhibitors extend themselves into an allosteric hydrophobic pocket adjacent to the ATP binding site and bind to the kinase in the "DFG-motif out" (inactive) conformation, which makes type-II inhibitors more active; moreover, given that the allosteric pocket residues are much less conserved between kinases, type-II inhibitors are therefore more selective as well.

One concern in the development of TRK kinase inhibitors is the potential risk of central nervous system (CNS) adverse events, regarding to their critical roles in the CNS normal function.[12-15] Unwanted adverse events related to the drug exposure in the CNS had been reported.[16] Therefore, the development of peripherally restricted TRK inhibitors is a rational and feasible approach to minimize the potential CNS toxicity.[17] Because of their binding modes, type-II kinase inhibitors generally bear a larger molecular weight and are more polar than type-I inhibitors, and are thus considered to be less permeable through the blood-brain barrier (BBB).[18-19] For example, the classical type-II BCR-ABL inhibitor imatinib (Gleevec®) exhibited excellent efficacy and safety profile and low CNS exposure.[20] In this context, the development of type-II TRKA inhibitors is highly desired. Currently, several type-II TRK inhibitors have been reported, but the majority of them are in the early discovery stage.[3, 21-23] One of the most advanced type-II TRKA inhibitor CE-245677 was discontinued in Phase I clinical trials;[17] its successor PF-06273340 completed the Phase I clinical trial in 2014, but no further progress was reported ever since.[24] Therefore, the exploitation of novel chemical scaffolds for type-II TRKA inhibitors is highly demanded.

As a part of our continuous effort on the development of kinase inhibitors,[25-30] especially TRKA inhibitors,[31] we recently screened a small in-house kinase compounds library, and compounds **1b** and **2b** were found to exhibit moderate TRKA inhibitory activity. Although thienopyrimidines derivatives had been reported having a variety of biological activities including anti-parasitic activity[32]; Bertrand *et al*, disclosed the co-crystal

structure of EX429 with TRKA and TRKB,[33] but the medicinal chemistry effort towards the discovery of this compound remained unknown. Therefore, we hypothesized that our thienopyrimidine derivativescould serve as a starting point for the discovery and development of novel TRK pan-inhibitors. From the initial hits **1b** and **2b**, utilizing the structure-based drug design (SBDD) approach, a series of potent TRKA inhibitors was designed and synthesized. The representative lead **4c** exhibited strong *in vitro* TRKA inhibition and anti-proliferative activity. In this paper, we report the design, synthesis, and biological evaluation of these compounds.

Results and discussion

Structure and activity relationship (SAR)

We quickly synthesized a few analogues of compounds **1b** and **2b** to explore the SAR of these two closely related scaffolds. Unfortunately, all compounds **1a-1c** and **2a-2c** were only moderately or weakly active in enzymatic and cellular assays (Tables 1 & 2). To understand the binding mode and further improve the potency, compounds **1b** and **2b** were docked to the TRKA protein (PDB ID: 6PL1). As shown in Figure 2A, compound **1b** bound to the TRKA protein in a classical type-II manner: a π-π interaction was found between the phenyl ring and Phe589, two hydrogen bonds with Glu560 and DFG-motif residue Asp668 were formed from the amide moiety, and the allosteric DFG pocket was occupied with the 3-(*tert*-butyl)-1-methyl-1*H*-pyrazole moiety; while in compound **2b**, a hydrogen bond from the N1 of 4-amino-thieno[3,2-*d*]pyrimidine was formed with the hinge region residue Met592 (Figure 2B). Compounds **1a-1c** features with the direct carbon-carbon connection between the phenyl ring and the thieno-pyrimidine core. Although the structural feature had been proved to be favored in a few kinase inhibitors (e.g. JAK inhibitor ruxolitinib and BTK inhibitor ibrutinib), [34] based on the molecular docking result, we discovered that this structural type is too rigid to have a strong binding with the TRKA kinase. In compounds **2a-2c**, the phenyl ring was bridged to the thieno-pyrimidine core through a nitrogen atom, which allows a flexible binding. As shown in the superimposed structures of **1b** and **2b** (Figure 2C), the spatial distance between the phenyl rings of **1b** and **2b** was only 1.8 Å. Therefore, we envisioned that a hybrid of these two scaffolds would be able to retain the original crucial interactions with the TRKA protein while maintaining a flexible binding for the optimal affinity.

Table 1. Structure-activity relationship of series **I** compounds.[a]

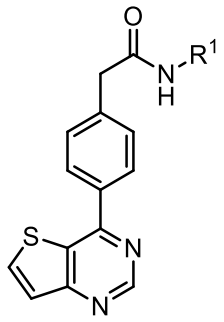

I

Compound	R^1	TRKA Inhibition % (@ 20 μM)[b]	KM12 cell IC_{50} (μM)
1a	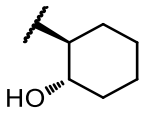	18.0	>200
1b	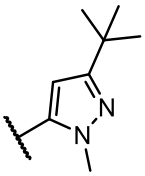	31.4	25.2 ± 4.8
1c	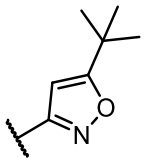	18.0	86.5 ± 11.2
Entrectinib	--	IC_{50}=0.0027 ± 0.0007 μM	0.014 ± 0.009

[a]IC_{50} values are shown as the mean ± SD of two independent assays.

[b]Inhibition percentage values are shown as the average of two independent assays.

Table 2. Structure-activity relationship of series **II** compounds.[a]

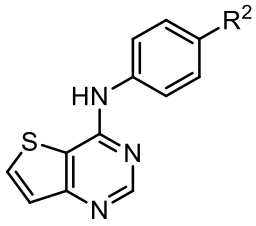

II

Compound	R^2	TRKA Inhibition % (@ 20 μM)[b]	KM12 cell IC_{50} (μM)
2a		18.0	102.6 ± 10.3

2b		17.4	132.8 ± 9.3
2c	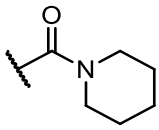	16.5	150.0 ± 11.6

[a]IC_{50} values are shown as the mean ± SD of two independent assays.

[b]Inhibition percentage values are shown as the average of two independent assays.

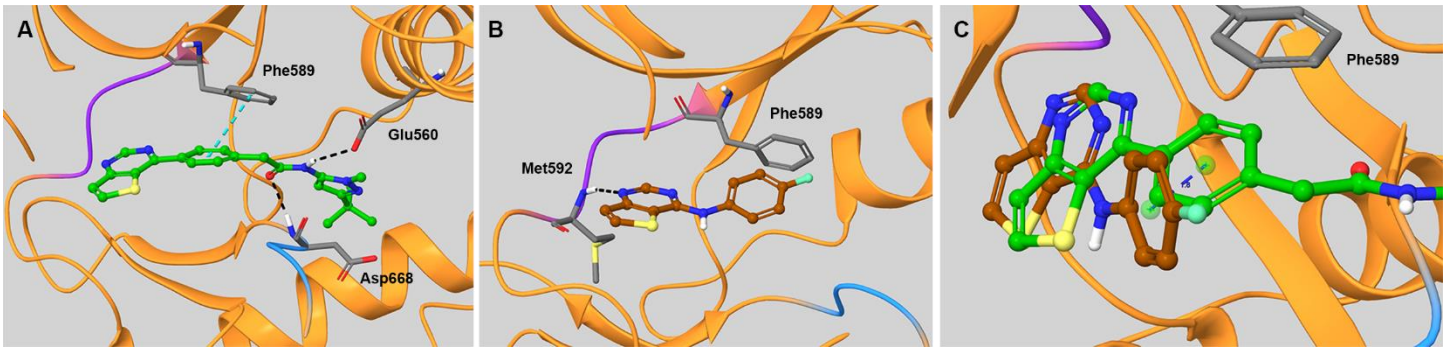

Figure 2. Proposed binding modes of **1b** and **2b** with TRKA. The protein structure of TRKA is shown as orange ribbon. The hinge region of TRKA is colored in violet, and the DFG-motif is colored in blue. Key residues are colored as follows: carbon grey, oxygen red, nitrogen blue, and hydrogen white. The hydrogen bonds are colored in black, and π-π interaction is colored in teal. (A) The atoms of **1b** are colored as follows: carbon green, oxygen red, nitrogen blue, sulfur yellow, and hydrogen white. (B) The atoms of **2b** are colored as follows: carbon brown, nitrogen blue, sulfur yellow, fluorine cyan, and hydrogen white. (C) Superimposed structures of **1b** and **2b**. Zoomed view on the phenyl rings.

Table 3. Structure-activity relationship of series **III** compounds.[a]

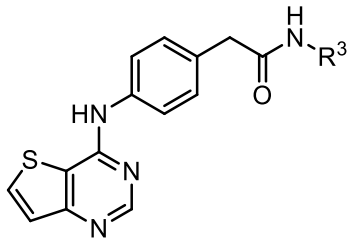

III

Compound	R^3	TRKA IC_{50} (μM)	KM12 cell IC_{50} (μM)

3a	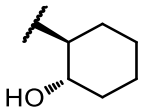	40.54 ± 8.84	>200
3b	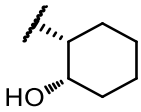	41.23 ± 1.90	>200
3c	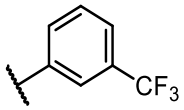	7.99 ± 0.58	14.36 ± 2.56
3d	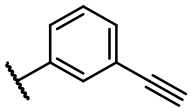	22.57 ± 3.47	38.83 ± 5.84
3e	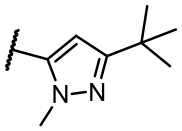	1.08 ± 0.04	18.77 ± 4.93
3f	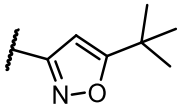	3.26 ± 0.25	16.50 ± 3.90
Entrectinib	--	0.0027 ± 0.0007	0.012 ± 0.00002

[a]IC_{50} values are shown as the mean ± SD of two independent assays.

A series of compounds were then synthesized and evaluated. The SAR study showed that the nature of R^3 group in the allosteric pocket had significant impacts on the activity (Table 3). Similar to that observed in the compound **1** series, aliphatic group substituted derivatives (**3a** and **3b**) were 2-40 fold less active than aromatic substituted derivatives (**3c**-**f**) in enzymatic assays, and the cellular potency was completely abolished. Among the aromatic substituted derivatives, the five-membered heterocyclic rings (**3e**-**f**) were more favored than substituted phenyls (**3c**-**d**). Moreover, the ethynyl derivative **3d** was about 3-fold less active than its trifluoromethyl analogue **3c**, probably due to a steric clash between the ethynyl fragment and the allosteric pocket residues. Compound **3e** was docked with TRKA (Figure 3). As expected, the π-π interaction between the phenyl acetamide fragment and the enzyme was retained, and a hydrogen bond was found between the hinge region residue Met592 and the N1 atom of compound **3e**.

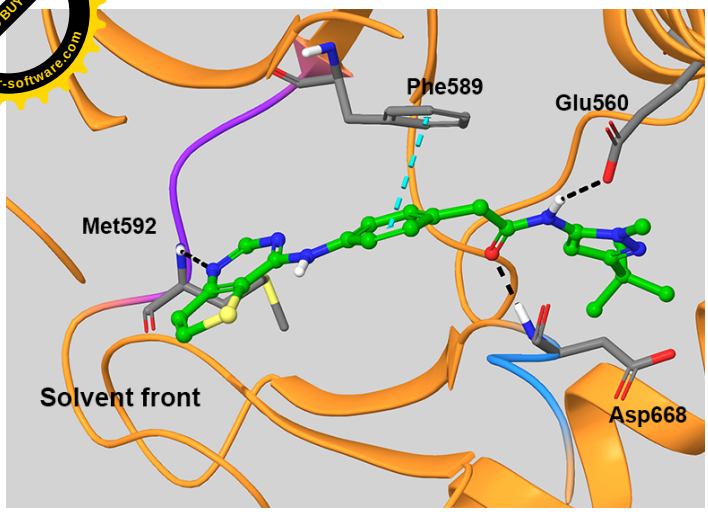

Figure 3. Proposed binding mode of compounds **3e** with TRKA. The protein structure of TRKA is shown as orange ribbon. The hinge region of TRKA is colored in violet, and the DFG-motif is colored in blue. Key residues are colored as follows: carbon grey, oxygen red, nitrogen blue, and hydrogen white. The hydrogen bonds are colored in black, and pi-pi interaction is colored in teal. The atoms of **3e** are colored as follows: carbon green, oxygen red, nitrogen blue, sulfur yellow, and hydrogen white.

Although compounds in the series **III** displayed excellent enzymatic potency in the low micromolar range, but the cellular potency was relatively weak. We envisioned that the low potency in cells could be due to poor aqueous solubility. As it was observed in the binding study of compound **3e** with TRKA kinase (Figure 3), the thiophenyl moiety of thieno-pyrimidine orients toward to the solvent front. We hypothesized that the introduction of a polar substituent group to the thiophenyl moiety could improve aqueous solubility while maintaining good ligand-protein interactions. Therefore, a methyl-pyrazole group was introduced to the 6-position of the thieno-pyrimidine moiety. To our delight, the resulting compounds **4a** and **4b** displayed approximately 10-fold increase in both enzymatic and cellular potencies than the parent compounds **3c** and **3d** (Table 3); strikingly, **4c** demonstrated a 20-fold improvement in enzymatic potency and 100-fold improvement in cellular potency than the parent compound **3e**.

Encouraged by these promising results, we proceeded to synthesize more derivatives to further explore SAR in the allosteric pocket. As shown in Table 3, the replacement of methyl-pyrazole in **4c** with thiazole (compound **4d**) resulted in 20- and 150-fold decreases in enzymatic and cellular potencies, respectively. Compound **4e** with morpholinoethyl attached to the pyrazole, exhibited a comparable enzymatic potency to **4c**; but was far less potent in the cellular assay. It can be explained with that the high polarity of compound **4e** limits its cell membrane permeability. Several compounds bearing a phenyl ring (**4f-h**) showed comparable cellular

potency with **4a** and **4b**, although compound **4h** was less active in the enzymatic assay than other compounds (**4a**-**g**). When the terminal phenyl group was replaced with a benzylic group (**4i**), a 25-fold drop in potency was observed (*vs* **4a**), indicating a potential steric clash with a surrounding residue; while a pyridine replacement (**4j**) resulted in a 70-fold decrease in enzymatic potency, probably due to an unfavored electrostatic interaction between pyridine and surrounding residues. Diaryl urea is an important pharmacophore in constructing type-II anticancer kinase inhibitors, exemplified by the success of sorafenib (Nexavar®). Therefore, compound **4k** bearing a urea linker was prepared and evaluated, which demonstrated comparable activities in both enzymatic and cellular levels as its amide partner **4c**.

Table 4. Structure-activity relationship of series **IV** compounds (part 1). [a]

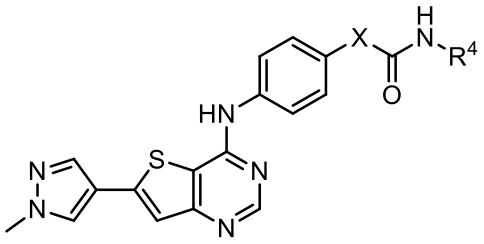

IV

Compound	X	R^4	TRKA IC_{50} (μM)	KM12 cell IC_{50} (μM)
4a	CH_2	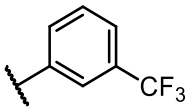	0.14 ± 0.03	1.49 ± 0.24
4b	CH_2	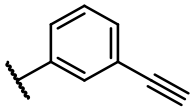	0.54 ± 0.07	1.42 ± 0.30
4c	CH_2	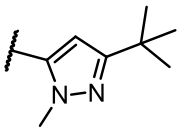	0.075 ± 0.001	0.14 ± 0.02
4d	CH_2	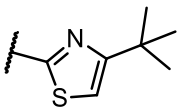	1.95 ± 0.19	20.92 ± 5.99
4e	CH_2	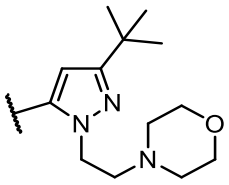	0.026 ± 0.001	1.65 ± 0.27

4f	CH_2	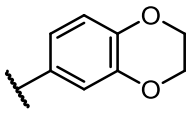	0.092 ± 0.054	1.02 ± 0.16
4g	CH_2	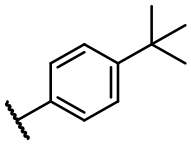	0.094 ± 0.016	0.09 ± 0.01
4h	CH_2	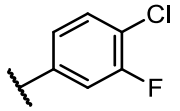	1.58 ± 0.17	1.38 ± 0.20
4i	CH_2	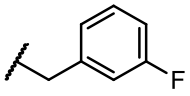	3.61 ± 0.34	>200
4j	CH_2	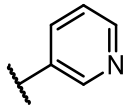	9.70 ± 1.59	ND[b]
4k	NH	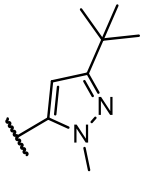	0.058 ± 0.008	0.13 ± 0.04
Entrectinib	--	--	0.0027 ± 0.0007	0.012 ± 0.00002

[a]IC_{50} values are shown as the mean ± SD of two independent assays.

[b]Not determined.

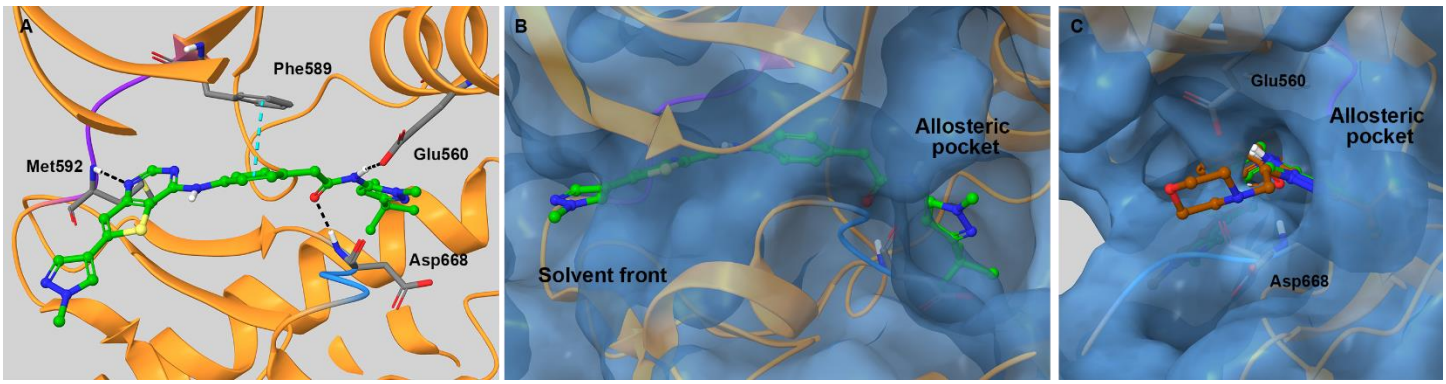

Figure 4. Proposed binding mode of compounds **4c** and **4e** with TRKA. The protein structure of TRKA is shown as orange ribbon. The hinge region of TRKA is colored in violet, and the DFG-motif is colored in blue. Key residues are colored as follows: carbon grey, oxygen red, nitrogen blue, and hydrogen white. The hydrogen bonds are colored in black. (A) The atoms of **4c** are colored as follows: carbon green, oxygen red, nitrogen blue, sulfur yellow, and hydrogen white. (B) The protein structure of TRKA is shown as an azure surface. (C)

Superimposed structures of **4c** and **4e**. The atoms of **4e** are colored as follows: carbon brown, oxygen red, nitrogen blue, sulfur yellow, and hydrogen white. Zoomed view on the morpholine moiety of **4e**.

As illustrated in the proposed binding mode of **4c** with the TRKA kinase (Figure 4A), all interactions observed between **3e** and the TRKA enzyme were retained with compound **4c**, with the terminal pyrazole group laying at the solvent front (Figure 4B). To rationalize the excellent enzymatic potency, compound **4e** was docked with the TRKA protein as well. Compound **4e** nicely superimposed with **4c**; meanwhile, the morpholine moiety of **4e** extended out of the allosteric hydrophobic pocket and was able to form a salt bridge with the carboxylic acid group of Glu560 or Asp668 (Figure 4C). This proposed binding mode explained its excellent enzymatic potency very well. The low potency could be explained with the low cell permeability of compound **4e**.

To explore the SAR in the R^5 region, the methyl-pyrazole was replaced (Table 5). 4-(Methylsulfonyl)phenyl group was established as a bioisosteric group of methyl-pyrazole which can avoid the formation of de-methylation metabolite.[28] However, the resulting compounds **4l** and **4m** totally abolished the potency in the enzymatic assay. Although it is unexpected, the loss of the potency can be partially explained with potential steric clash between the bulky methylsulfonyl (**4l**) or trimethoxyl group (**4m**) with surrounding residues; because as observed in Figure 4B, the methyl-pyrazole of **4c** was tightly surrounded by the solvent front residues. In line with the above speculation, a less hindered pyrrolidin-ethoxy-phenyl group was well tolerated and compound **4n** displayed a comparable enzymatic and cellular potency to compound **4h**. The tolerability of a solubilizing group from the pyrazole moiety is an important SAR discovery which would enable the further optimization of solubility and drug properties.

Table 5. Structure-activity relationship of series **IV** compounds (part 2). [a]

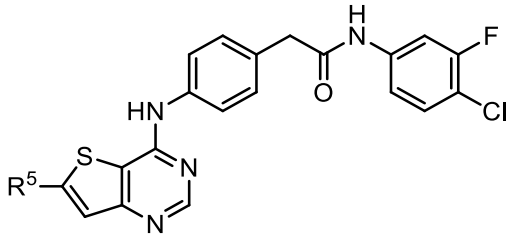

IV

Compound	R^5	TRKA IC_{50} (μM)	KM12 cell IC_{50} (μM)

4h	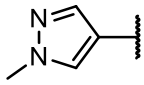	1.58 ± 0.17	1.38 ± 0.20
4l	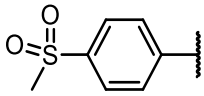	~200	ND[b]
4m	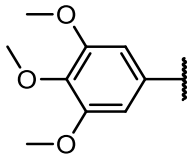	>200	ND[b]
4n	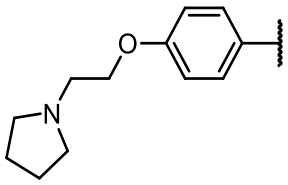	0.23 ± 0.07	1.26 ± 0.11

[a]IC_{50} values are shown as the mean ± SD of two independent assays.
[b]Not determined.

Western Blot

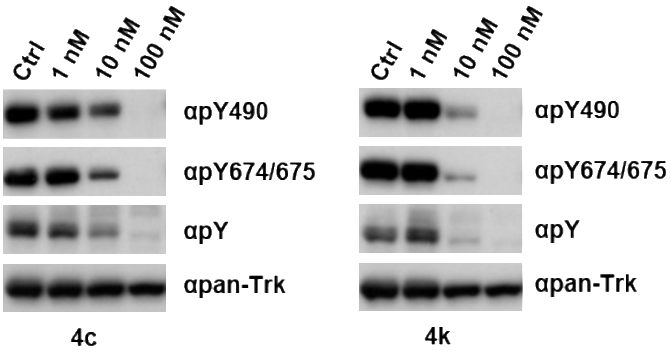

Figure 5. Inhibition of TPM3-TRKA phosphorylation by **4c**, and **4k** in human colorectal carcinoma derived cell line KM12. KM12 cell line were serum starved and treated for 2 hours with the indicated concentrations of the compounds. Total cell lysates (50 µg) were subjected to immunoblotting with anti-phospho-TRKA (αpY490 and αpY4674/675) and anti-phospho-Tyrosine (αpY) antibodies. The blots were normalized using anti-TRK (αpan-TRK) antibody.

In order to explore the ability of these new compounds to inhibit TRK-derived oncoproteins in cells, we analyzed their effects on the phosphorylation of TRKA using the human colorectal cancer derived cell line KM12 which endogenously harbours TPM3-TRKA rearrangement. As shown in Figure 5, compounds **4c** and **4k** inhibited the TPM3-TRKA autophosphorylation in a dose-dependent manner. Both compounds completely inhibited TPM3-TRKA autophosphorylation at the concentration of 100 nM; while **4k** was able to significantly

inhibit the TPM3-TRKA autophosphorylation on Y490 and Y674/Y675 at the concentration of 10 nM. These results suggested that both compounds **4c** and **4k** exhibited an effective blockage of the TRKA autophosphorylation with a relatively low concentration in cells, which is correlated with the anti-proliferative activity.

Table 6. Kinase selectivity profile of compound **4c**. [a]

Kinase	IC_{50} (μM)
TRKA	0.075 ± 0.001
TRKB	0.074 ± 0.007
TRKC	0.055 ± 0.014
Aurora A	0.893 ± 0.006
Aurora B	1.99 ± 0.24
CSF-1R	13.6 ± 0.3
MAP4K4	41.5 ± 7.8
EGFR	176.09 ± 18.21
NEK2	>200

[a] IC_{50} values are shown as the mean ± SD of two independent assays.

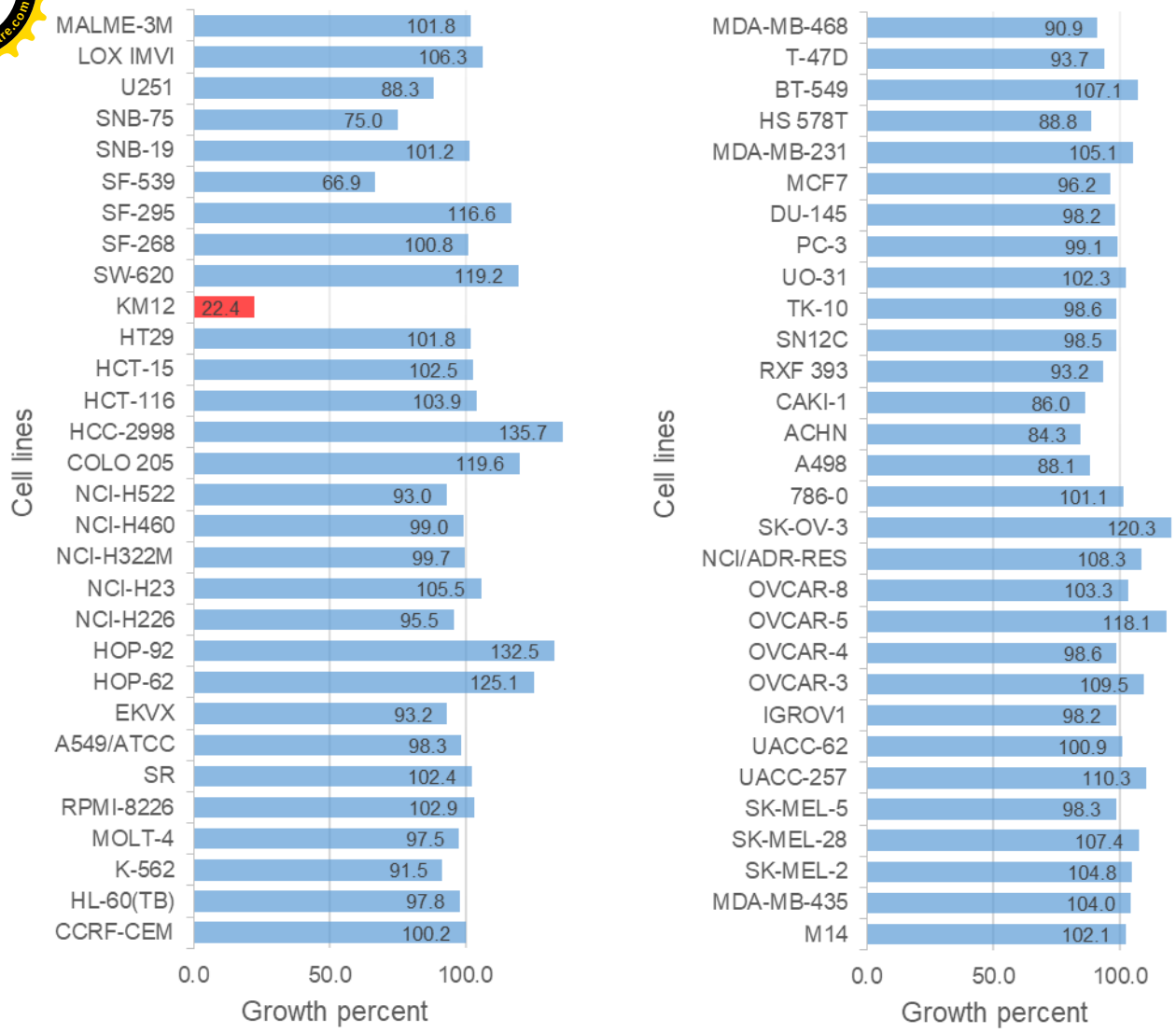

Figure 6. NCI-60 human cancer cell lines screen of compound **4g**.

Selectivity profile

To assess the selectivity of our compounds, inhibitory activities of **4c** and **4g** were tested against a panel of kinases and NCI-60 human cancer cell lines, respectively. As shown in Table 6, **4c** exhibited pan-TRK inhibitory activity and was almost equal potent against TRKA-C, but was much less active against other kinases. Furthermore, as illustrated in Figure 6, **4g** also exhibited excellent selectivity against TRKA-driven KM12 cells. At the drug concentration of 10 μM, **4g** demonstrated nearly 80% of growth inhibition for KM12, while only minimal inhibitory activity was observed for the remaining 59 cancer cell lines. These data indicated our compounds are selective against TRK oncogenes at both enzymatic and cellular levels.

Blood-brain barrier permeability

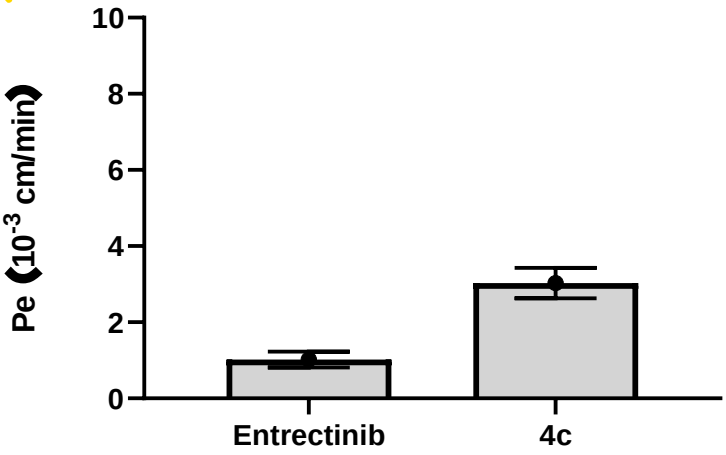

Figure 7. Transport assessment of entrectinib and **4c** across *in vitro* BBB model.

To evaluate the BBB permeability, entrectinib and **4c** were subjected to the *in vitro* BBB transport assay. As shown in Figure 7, the diffusion of entrectinib (permeability coefficient (Pe) = 1.02 x 10^{-3} cm/min) across the BBB was observed in our human *in vitro* BBB model, which was in line with published data that entrectinib crossed the BBB in the mouse xenograft model.[35] Compound **4c** (Pe = 3.03 × 10^{-3} cm/min) was more permeable than entrectinib, which was predicted from its lower molecular weight (500.6 Da *vs* 560.6 Da of entrectinib) and higher predicted LogP (5.15 *vs* 4.45 of entrectinib). We envisioned that by strategically increasing molecular weight and lowing LogP could lead to the discovery of derivatives having desirable cancer cell killing activity and low BBB permeability.

Chemistry

As shown in Scheme 1, the key intermediates acids **7**, **11**, **14**, and **15** were synthesized through either a telescope coupling-hydrolysis reaction (**7** and **14**) or a successive substitution-hydrolysis reaction (**11** and **15**). Final compounds **1**, **3**, and **4a-j** were synthesized from the corresponding acids and amines using HATU as the acylation reagent in DMF at room temperature; amide **16** was synthesized from acid **15** following the same procedure, and then compound **16** was coupled with the corresponding boronic acids to give final compounds **4l-n**. Compounds **12** and **17** were irradiated under microwave to produce **18**, which underwent a successive coupling and de-protection procedure to generate amine **19**. Urea compound **4k** was prepared from aniline **19** and 3-(*tert*-butyl)-1-methyl-1*H*-pyrazol-5-amine in the presence of triphosgene. To synthesize intermediate **24**, **20** was reacted with an excessive amount of TsCl to give compound **21**; compound **21** was heated in morpholine

to give compound **22**, but the self-cyclized product **23** was also isolated in 30% yield, which was not expected since the amino group was hindered by the bulky Ts groups. The Ts-protection group was removed by stirring to give compound **24** in H_2SO_4 at ambient temperature. Amine **24** was too hydrophilic to be extracted from water. Therefore, the reaction mixture was concentrated after base quenching, and the resulting crude was used directly for next step without purification.

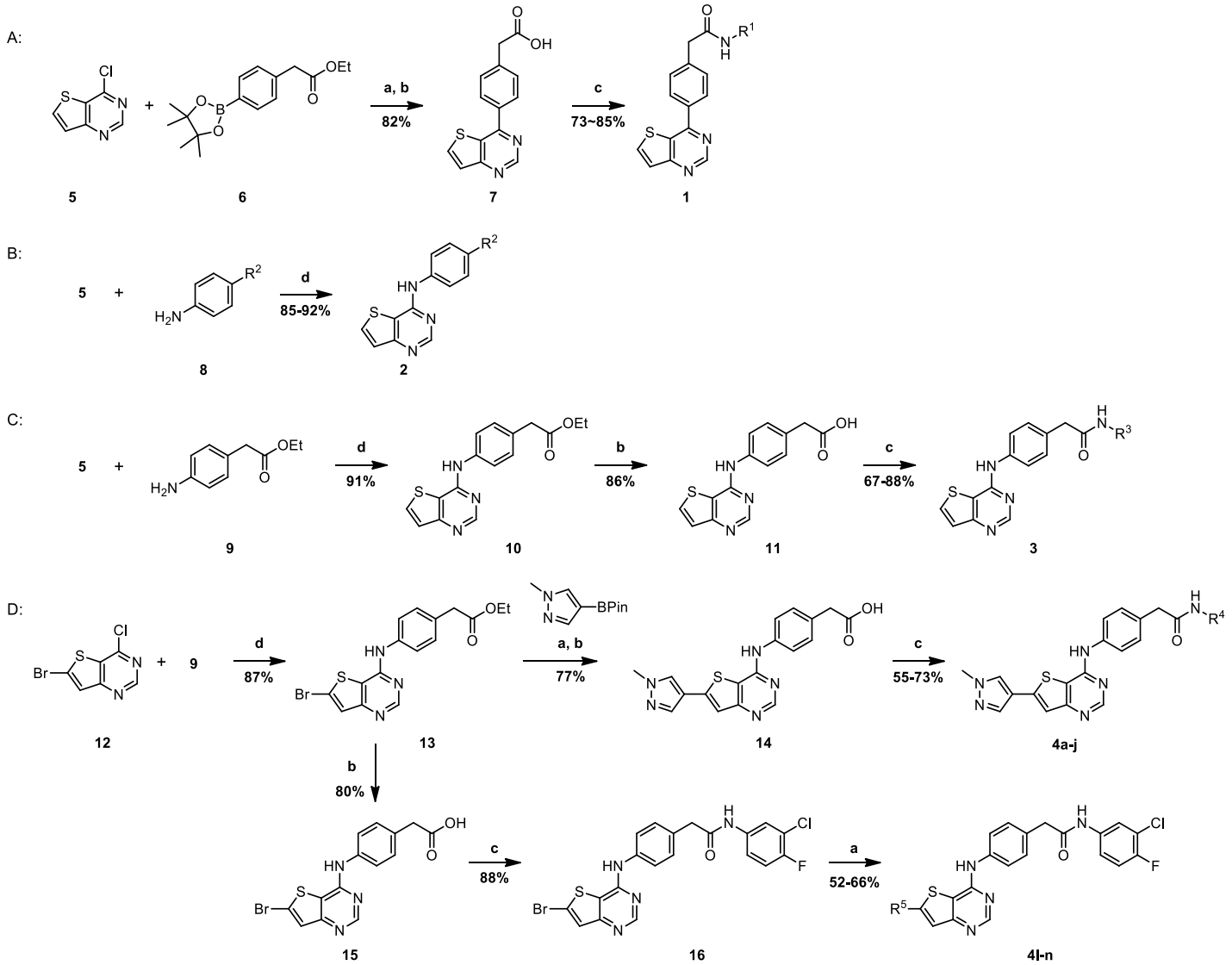

Scheme 1. Synthesis of final compounds. Reagents and conditions: (a) $Pd(PPh_3)_4$, $NaHCO_3$, THF, H_2O, microwave, 140 °C, 0.5 h; (b) LiOH, THF, H_2O, microwave, 80 °C, 0.5 h; (c) amines, HATU, Et_3N, DMF, R.T., overnight; (d) ^{i}PrOH, microwave, 100 °C, 0.5 h.

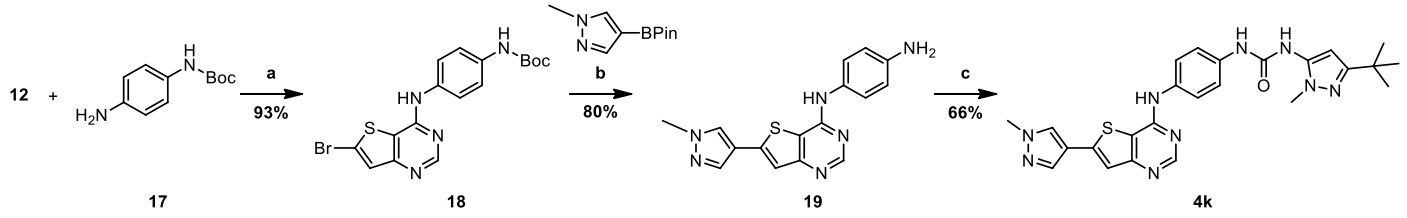

Scheme 2. Synthesis of compound **4k**. Reagents and conditions: (a) ^{i}PrOH, microwave, 100 °C, 0.5 h; (i) (i) [illegible] $Pd(PPh_3)_4$, $NaHCO_3$, THF, H_2O, microwave, 140 °C, 0.5 h; (ii) TFA, DCM, R.T., 2 h; (c) (i) 3-(*tert*-butyl)-1-methyl-1*H*-pyrazol-5-amine, triphosgene, Et_3N, DCM, 0 °C to R.T., 2 h. (ii) **19**, DCM, R.T., overnight.

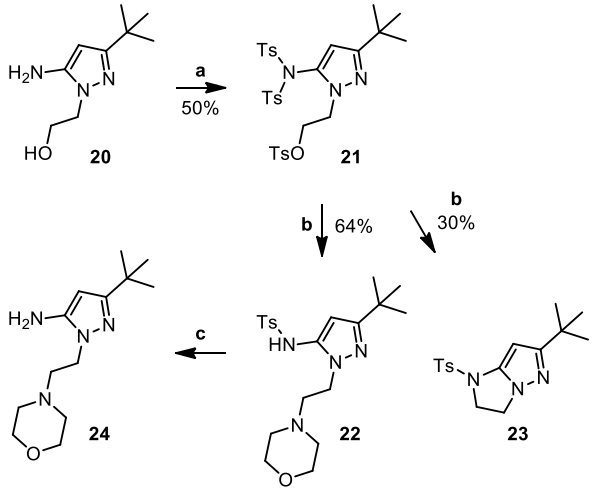

Scheme 3. Synthesis of intermediate **24**. Reagents and conditions: (a) TsCl, Et_3N, DCM, R.T. to reflux, overnight; (b) morpholine, 120 °C, overnight; (c) H_2SO_4, R.T., overnight.

Conclusion

In summary, we have discovered a novel series of 2-(4-(thieno[3,2-*d*]pyrimidin-4-ylamino)phenyl)acetamide derivatives as potent TRKA inhibitors. By utilizing the SBDD strategy, compound **4c** was identified through the optimization of the starting hits **1** and **2**. Compound **4c** exhibited excellent *in vitro* TRKA, TRKB, and TRKC kinase inhibitory and anti-proliferative activities in the TRKA driven cell line. In the NCI-60 human cancer cell lines screen, compound **4g** demonstrated nearly 80% of growth inhibition for KM12, while only minimal inhibitory activity was observed for the remaining 59 cancer cell lines at 10 μM. Western blot analysis indicated that compounds **4c** and **4k** suppressed the TPM3-TRKA autophosphorylation at 10-100 nM concentration, implying that the inhibitory activity in cells was derived from the inhibition of TRKA. Molecular modeling study demonstrated that this series of compounds bond to the TRKA kinase in a type-II manner. The work presented provided convincing evidence that 2-(4-(thieno[3,2-*d*]pyrimidin-4-ylamino)phenyl)acetamides could serve as a novel scaffold for the discovery and development of potent and selective type-II TRK inhibitors.

Experimental Section

Chemistry.

All starting materials and reagents were either obtained from commercial suppliers or prepared according to literature reported procedures. All purchased chemicals and solvents were used without further purification

unless otherwise noted. Flash chromatography was performed using silica gel (300−400 mesh) on Teledyne ISCO CombiFlash. All reactions were monitored by thin-layer chromatography (TLC) or liquid chromatography mass spectrometry (LC-MS) (Thermo Surveyor HPLC System with Thermo Finnigan LCQ Deca). ^{1}H NMR spectral data were recorded on Varian 400 NMR spectrometer, and ^{13}C NMR was recorded on Varian Mercury 101 NMR spectrometer at ambient temperature. Chemicals shifts (δ) were reported in parts per million, coupling constants (*J*) values were in hertz, and the splitting patterns were abbreviated as follows: s for singlet; d for doublet; t for triplet; q for quartet; and m for multiplet. All final compounds for biological evaluation were purified to ≥95% purity as determined by Agilent 1100 HPLC instrument (column: Phenomenex kinetex 150 × 4.6 mm, 5 μm; solvent A: H_2O/0.1% TFA; solvent B: MeOH/0.1% TFA; run time 12 min.; time/%B: 0.0/30, 6.0/100, 7.0/100, 7.01/30,12.0/30; flow rate: 0.8 mL/min.; wavelength: 254 nm).

General procedure A*: *Synthesis of compounds 1, 3, 4a-j, and 16. Acids such as **7**, **11**, **14,** or **15** (0.14 mmol), amine (0.16 mmol), HATU (0.16 mmol), and Et_3N (0.28 mmol) were dissolved in anhydrous DMF (1 mL). The reaction mixture was stirred at ambient temperature overnight. The completion of the reaction was monitored by LC-MS analysis. The reaction mixture was poured into water and extracted with ethyl acetate. The organic phase was washed with water and brine twice, and concentrated in vacuum. The resulting residue was purified by silica gel chromatography to get the title compound.

*N-((1R,2R)-2-hydroxycyclohexyl)-2-(4-(thieno[3,2-d]pyrimidin-4-yl)phenyl)acetamide (**1a**)*. The title compound was synthesized from **7** and (1*R*,2*R*)-2-aminocyclohexanol hydrochloride following general procedure A. White solid (73%). ^{1}H NMR (400 MHz, DMSO-d_6) δ 9.25 (s, 1H), 8.56 (d, *J* = 5.5 Hz, 1H), 8.12 (d, *J* = 7.9 Hz, 2H), 7.81 (d, *J* = 8.0 Hz, 1H), 7.72 (d, *J* = 5.6 Hz, 1H), 7.54 (d, *J* = 8.0 Hz, 2H), 4.62 (d, *J* = 3.8 Hz, 1H), 3.74 (s, 1H), 3.71 – 3.62 (m, 1H), 3.61 (s, 2H), 1.71 – 1.49 (m, 4H), 1.47 – 1.36 (m, 2H), 1.33 – 1.17 (m, 2H). ^{13}C NMR (101 MHz, DMSO-d_6) δ 168.86, 161.87, 158.81, 154.58, 140.37, 138.43, 134.71, 129.79, 128.07, 127.15, 124.44, 66.82, 50.87, 42.09, 31.69, 26.63, 23.76, 19.57. LC-MS (ESI) *m/z*: $[M + H]^+$ 368.1. HPLC purity: 100%, t_R (retention time) = 6.87 min.

*N-(3-(tert-butyl)-1-methyl-1H-pyrazol-5-yl)-2-(4-(thieno[3,2-d]pyrimidin-4-yl)phenyl)acetamide (**1b**)*. The title compound was synthesized from **7** and 3-(*tert*-butyl)-1-methyl-1*H*-pyrazol-5-amine following general procedure A. White solid (82%). ^{1}H NMR (400 MHz, DMSO-d_6) δ 10.15 (s, 1H), 9.27 (s, 1H), 8.57 (d, *J* = 5.5 Hz, 1H), 8.17 (d, *J* = 7.0 Hz, 2H), 7.73 (d, *J* = 5.5 Hz, 1H), 7.61 (d, *J* = 7.2 Hz, 2H), 6.08 (s, 1H), 3.84 (s, 2H), 3.61 (s, 3H),

1.19 (s, 9H). ^{13}C NMR (101 MHz, DMSO-d_6) δ 168.44, 161.91, 158.72, 158.62, 154.60, 139.05, 138.50, 136.17, 135.12, 129.98 (2C), 128.26 (2C), 127.21, 124.46, 94.96, 41.91, 35.30, 31.77, 30.30 (3C). LC-MS (ESI) *m/z*: $[M + H]^+$ 406.3. HPLC purity: 100%, t_R = 7.53 min.

*N-(5-(tert-butyl)isoxazol-3-yl)-2-(4-(thieno[3,2-d]pyrimidin-4-yl)phenyl)acetamide (**1c**).* The title compound was synthesized from **7** and 5-(*tert*-butyl)isoxazol-3-amine following general procedure A. White solid (85%). ^{1}H NMR (400 MHz, DMSO-d_6) δ 11.28 (s, 1H), 9.26 (d, *J* = 1.1 Hz, 1H), 8.57 (d, *J* = 5.6 Hz, 1H), 8.15 (d, *J* = 7.5 Hz, 2H), 7.73 (d, *J* = 5.5 Hz, 1H), 7.59 (d, *J* = 7.8 Hz, 2H), 6.59 (s, 1H), 3.83 (s, 2H), 1.27 (s, 9H). ^{13}C NMR (101 MHz, DMSO-d_6) δ 180.47, 168.94, 161.90, 158.71, 157.87, 154.59, 138.67, 138.50, 135.21, 130.00 (2C), 128.27 (2C), 127.23, 124.45, 93.12, 42.26, 32.47, 28.29 (3C). LC-MS (ESI) *m/z*: $[M + H]^+$ 393.3. HPLC purity: 97.9%, t_R = 8.02 min.

*N-((1S,2S)-2-hydroxycyclohexyl)-2-(4-(thieno[3,2-d]pyrimidin-4-ylamino)phenyl)acetamide (**3a**).* The title compound was synthesized from **11** and (1*R*,2*R*)-2-aminocyclohexanol hydrochloride following general procedure A. Beige solid (67%). ^{1}H NMR (400 MHz, DMSO-d_6) δ 9.64 (s, 1H), 8.55 (d, *J* = 1.8 Hz, 1H), 8.21 – 8.18 (m, 1H), 7.68 – 7.64 (m, 2H), 7.62 (d, *J* = 8.1 Hz, 1H), 7.45 (d, *J* = 5.4 Hz, 1H), 7.25 (d, *J* = 8.3 Hz, 2H), 4.61 – 4.56 (m, 1H), 3.71 (s, 1H), 3.64 (s, 1H), 3.45 (s, 2H), 1.70 – 1.47 (m, 4h), 1.46 – 1.34 (m, 2H), 1.31 – 1.16 (m, 2H). ^{13}C NMR (101 MHz, DMSO-d_6) δ 169.48, 160.33, 155.27, 154.02, 137.18, 134.14, 132.13, 129.03 (2C), 124.34, 122.28 (2C), 115.28, 66.86, 50.77, 41.79, 39.52, 31.72, 26.64, 23.77, 19.56. LC-MS (ESI) *m/z*: $[M + H]^+$ 383.3. HPLC purity: 100%, t_R = 5.26 min.

*N-((1R,2S)-2-hydroxycyclohexyl)-2-(4-(thieno[3,2-d]pyrimidin-4-ylamino)phenyl)acetamide (**3b**).* The title compound was synthesized from **11** and (1*R*,2*S*)-2-aminocyclohexanol following general procedure A. Beige solid (70%). ^{1}H NMR (400 MHz, DMSO-d_6) δ 9.64 (s, 1H), 8.54 (s, 1H), 8.23 – 8.18 (m, 1H), 7.65 (d, *J* = 8.4 Hz, 2H), 7.62 (d, *J* = 8.1 Hz, 1H), 7.45 (d, *J* = 5.4 Hz, 1H), 7.25 (d, *J* = 8.3 Hz, 2H), 4.59 (d, *J* = 3.9 Hz, 1H), 3.71 (s, 1H), 3.63 (t, *J* = 8.6 Hz, 1H), 3.44 (s, 2H), 3.19 – 3.14 (m, 1H), 1.70 – 1.18 (m, 7H). ^{13}C NMR (101 MHz, DMSO-d_6) δ 169.47, 160.33, 155.27, 154.02, 137.18, 134.15, 132.14, 129.02 (2C), 124.35, 122.27 (2C), 115.27, 66.85, 50.76, 41.78, 31.72, 26.64, 23.76, 19.56. LC-MS (ESI) *m/z*: $[M + H]^+$ 383.4. HPLC purity: 100%, t_R = 5.34 min.

*2-(4-[illegible]ieno[3,2-d]pyrimidin-4-ylamino)phenyl)-N-(3-(trifluoromethyl)phenyl)acetamide (**3c**).* The title compound was synthesized from **11** and 3-(trifluoromethyl)aniline following general procedure A. Beige solid (88%). ^{1}H NMR (400 MHz, DMSO-d_6) δ 10.50 (s, 1H), 9.69 (s, 1H), 8.56 (s, 1H), 8.21 (d, J = 5.4 Hz, 1H), 8.12 (s, 1H), 7.81 (d, J = 8.2 Hz, 1H), 7.72 (d, J = 8.2 Hz, 2H), 7.55 (t, J = 8.0 Hz, 1H), 7.46 (d, J = 5.4 Hz, 1H), 7.39 (d, J = 7.7 Hz, 1H), 7.34 (d, J = 8.2 Hz, 2H), 3.68 (s, 2H). ^{13}C NMR (101 MHz, DMSO-d_6) δ 169.85, 160.32, 155.24, 153.99, 139.95, 137.66, 134.19, 130.76, 129.96, 129.44 (q, J = 32 Hz), 129.21 (2C), 124.09 (q, J = 272 Hz), 124.34, 122.60, 122.31 (2C), 119.52 (q, J = 4 Hz), 115.37, 115.11 (q, J = 4 Hz), 42.78. LC-MS (ESI) *m/z*: $[M + H]^+$ 429.0. HPLC purity: 99.5%, t_R = 6.72 min.

*N-(3-ethynylphenyl)-2-(4-(thieno[3,2-d]pyrimidin-4-ylamino)phenyl)acetamide (**3d**).* The title compound was synthesized from **11** and 3-ethynylaniline following general procedure A. Beige solid (83%). ^{1}H NMR (400 MHz, DMSO-d_6) δ 10.27 (s, 1H), 9.69 (s, 1H), 8.56 (s, 1H), 8.20 (d, J = 5.4 Hz, 1H), 7.82 (s, 1H), 7.72 (d, J = 8.3 Hz, 2H), 7.59 (d, J = 8.3 Hz, 1H), 7.46 (d, J = 5.4 Hz, 1H), 7.37 – 7.28 (m, 3H), 7.15 (d, J = 7.6 Hz, 1H), 4.16 (s, 1H), 3.65 (s, 2H). ^{13}C NMR (101 MHz, DMSO-d_6) δ 169.51, 160.34, 155.24, 154.00, 139.41, 137.59, 134.17, 130.97, 129.18, 129.16 (2C), 126.43, 124.35, 122.32 (2C), 122.00, 121.94, 119.69, 115.35, 83.35, 80.51, 42.79. LC-MS (ESI) *m/z*: $[M + H]^+$ 385.1. HPLC purity: 99.2%, t_R = 6.18 min.

*N-(3-(tert-butyl)-1-methyl-1H-pyrazol-5-yl)-2-(4-(thieno[3,2-d]pyrimidin-4-ylamino)phenyl)acetamide (**3e**).* The title compound was synthesized from **11** and 3-(*tert*-butyl)-1-methyl-1*H*-pyrazol-5-amine following general procedure A. Beige solid (72%). ^{1}H NMR (400 MHz, DMSO-d_6) δ 10.03 (s, 1H), 9.68 (s, 1H), 8.56 (s, 1H), 8.21 (d, J = 5.4 Hz, 1H), 7.72 (d, J = 7.9 Hz, 2H), 7.46 (d, J = 5.4 Hz, 1H), 7.33 (d, J = 8.0 Hz, 2H), 6.06 (s, 1H), 3.66 (s, 2H), 3.58 (s, 3H), 1.19 (s, 9H). ^{13}C NMR (101 MHz, DMSO-d_6) δ 169.10, 160.37, 158.60, 155.24, 154.01, 137.62, 136.27, 134.19, 130.85, 129.15 (2C), 124.36, 122.30 (2C), 115.36, 95.02, 41.64, 35.27, 31.78, 30.32 (3C). LC-MS (ESI) *m/z*: $[M + H]^+$ 421.2. HPLC purity: 100%, t_R = 6.15 min.

*N-(5-(tert-butyl)isoxazol-3-yl)-2-(4-(thieno[3,2-d]pyrimidin-4-ylamino)phenyl)acetamide (**3f**).* The title compound was synthesized from **11** and 5-(*tert*-butyl)isoxazol-3-amine following general procedure A. Beige solid (69%). ^{1}H NMR (400 MHz, DMSO-d_6) δ 11.17 (s, 1H), 9.68 (s, 1H), 8.55 (s, 1H), 8.21 (dd, J = 5.4, 1.3 Hz, 1H), 7.70 (d, J = 7.4 Hz, 2H), 7.45 (dd, J = 5.4, 1.3 Hz, 1H), 7.30 (d, J = 7.7 Hz, 2H), 6.58 (s, 1H), 3.65 (s, 2H), 1.27 (s, 9H). ^{13}C NMR (101 MHz, DMSO-d_6) δ 180.40, 169.54, 160.36, 157.94, 155.22, 153.99, 137.68, 134.19,

130.[illegible], 129.17 (2C), 124.35, 122.31(2C), 115.35, 93.10, 41.98, 32.47, 28.31(3C). LC-MS (ESI) *m/z*: [M + H]$^+$ [illegible].1. HPLC purity: 99.2%, t_R = 6.56 min.

*2-(4-((6-(1-methyl-1H-pyrazol-4-yl)thieno[3,2-d]pyrimidin-4-yl)amino)phenyl)-N-(3-(trifluoromethyl)phenyl)acetamide (**4a**).* The title compound was synthesized from **14** and 3-(trifluoromethyl)aniline following general procedure A. Beige solid (62%). ^{1}H NMR (400 MHz, DMSO-d_6) δ 10.50 (s, 1H), 9.60 (s, 1H), 8.51 (s, 1H), 8.28 (s, 1H), 8.12 (s, 1H), 7.96 (s, 1H), 7.81 (d, *J* = 8.3 Hz, 1H), 7.71 (d, *J* = 8.3 Hz, 2H), 7.57 – 7.52 (m, 2H), 7.39 (d, *J* = 7.8 Hz, 1H), 7.33 (d, *J* = 8.3 Hz, 2H), 3.91 (s, 3H), 3.67 (s, 2H). ^{13}C NMR (101 MHz, DMSO-d_6) δ 169.88, 161.21, 154.56, 154.29, 141.85, 139.96, 137.79, 136.90, 130.56, 129.97,129.44 (q, *J* = 32 Hz), 129.22 (2C), 129.18, 124.09 (q, *J* = 272 Hz), 122.61, 122.08 (2C), 119.52 (q, *J* = 4 Hz), 118.22, 115.31, 115.11 (q, *J* = 4 Hz), 113.20, 54.89, 42.79. LC-MS (ESI) *m/z*: [M + H]$^+$ 509.2. HPLC purity: 99.4%, t_R = 6.96 min. HRMS (ESI) *m/z*: [M + H]$^+$ calcd for $C_{25}H_{20}F_3N_6OS$ 509.1371; found 509.1354.

*N-(3-ethynylphenyl)-2-(4-((6-(1-methyl-1H-pyrazol-4-yl)thieno[3,2-d]pyrimidin-4-yl)amino)phenyl)acetamide (**4b**).* The title compound was synthesized from **14** and 3-ethynylaniline following general procedure A. Beige solid (73%). ^{1}H NMR (400 MHz, DMSO-d_6) δ 10.26 (s, 1H), 9.59 (s, 1H), 8.51 (s, 1H), 8.28 (s, 1H), 7.96 (s, 1H), 7.81 (s, 1H), 7.70 (d, *J* = 7.6 Hz, 2H), 7.59 (d, *J* = 7.6 Hz, 1H), 7.54 (d, *J* = 1.1 Hz, 1H), 7.31 (dd, *J* = 7.4, 5.1 Hz, 3H), 7.17 – 7.12 (m, 1H), 4.16 (s, 1H), 3.91 (s, 3H), 3.64 (s, 2H). ^{13}C NMR (101 MHz, DMSO-d_6) δ 169.53, 161.21, 154.57, 154.30, 141.83, 139.42, 137.72, 136.90, 130.78, 129.19, 129.16 (2C), 126.42, 122.09 (2C), 121.99, 121.93, 119.68, 118.21, 115.31, 113.18, 83.35, 80.51, 42.79, 38.83. LC-MS (ESI) *m/z*: [M + H]$^+$ 465.2. HPLC purity: 98.8%, t_R = 6.54 min. HRMS (ESI) *m/z*: [M + H]$^+$ calcd for $C_{26}H_{21}N_6OS$ 465.1498; found 465.1491.

*N-(3-(tert-butyl)-1-methyl-1H-pyrazol-5-yl)-2-(4-((6-(1-methyl-1H-pyrazol-4-yl)thieno[3,2-d]pyrimidin-4-yl)amino)phenyl)acetamide (**4c**).* The title compound was synthesized from **14** and 3-(*tert*-butyl)-1-methyl-1*H*-pyrazol-5-amine following general procedure A. White solid (58%). ^{1}H NMR (400 MHz, DMSO-d_6) δ 10.03 (s, 1H), 9.60 (s, 1H), 8.52 (s, 1H), 8.29 (s, 1H), 7.96 (s, 1H), 7.70 (d, *J* = 7.7 Hz, 2H), 7.54 (s, 1H), 7.32 (d, *J* = 7.9 Hz, 2H), 6.06 (s, 1H), 3.91 (s, 3H), 3.66 (s, 2H), 3.58 (s, 3H), 1.19 (s, 9H). ^{13}C NMR (101 MHz, DMSO-d_6) δ 169.10, 161.13, 158.59, 154.57, 154.26, 141.88, 137.70, 136.90, 136.26, 130.69, 129.18, 129.15 (2C), 122.10

(2C), 118.16, 115.28, 113.16, 95.01, 41.62, 38.82, 35.27, 31.77, 30.31 (3C). LC-MS (ESI) *m/z*: [M + H]$^+$ [illegible]. HPLC purity: 100%, t_R = 7.02 min. HRMS (ESI) *m/z*: [M + H]$^+$ calcd for $C_{26}H_{29}N_8OS$ 501.2185; found 501.2174.

*N-(4-(tert-butyl)thiazol-2-yl)-2-(4-((6-(1-methyl-1H-pyrazol-4-yl)thieno[3,2-d]pyrimidin-4-yl)amino)phenyl)acetamide (**4d**).* The title compound was synthesized from **14** and 4-(*tert*-butyl)thiazol-2-amine following general procedure A. Yellow solid (62%). ^{1}H NMR (400 MHz,DMSO-d_6) δ 12.30 (s, 1H), 9.59 (s, 1H), 8.51 (s, 1H), 8.28 (s, 1H), 7.96 (s, 1H), 7.69 (d, *J* = 8.3 Hz, 2H), 7.54 (s, 1H), 7.31 (d, *J* = 8.3 Hz, 2H), 3.91 (s, 3H), 3.73 (s, 2H), 1.26 (s, 9H). ^{13}C NMR (101 MHz, DMSO-d_6) δ 169.24, 161.21, 160.12, 157.15, 154.54, 154.28, 141.85, 137.88, 136.89, 130.06, 129.25 (2C), 129.17, 122.11 (2C), 118.20, 115.29, 113.18, 104.60, 41.16, 38.82, 34.10, 29.75 (3C). LC-MS (ESI) *m/z*: [M + H]$^+$ 504.1. HPLC purity: 95.7%, t_R = 7.28 min. HRMS (ESI) *m/z*: [M + H]$^+$ calcd for $C_{25}H_{26}N_7OS_2$ 504.1640; found 504.1635.

*N-(3-(tert-butyl)-1-(2-morpholinoethyl)-1H-pyrazol-5-yl)-2-(4-((6-(1-methyl-1H-pyrazol-4-yl)thieno[3,2-d]pyrimidin-4-yl)amino)phenyl)acetamide (**4e**).* The title compound was synthesized from **14** and **25** following general procedure A. Beige solid (55%). ^{1}H NMR (400 MHz, DMSO-d_6) δ 10.26 (s, 1H), 9.79 (s, 1H), 8.71 (s, 1H), 8.48 (s, 1H), 8.16 (s, 1H), 7.93 (d, *J* = 8.3 Hz, 2H), 7.74 (s, 1H), 7.52 (d, *J* = 8.3 Hz, 2H), 6.26 (s, 1H), 4.18 (t, *J* = 7.0 Hz, 2H), 4.10 (s, 3H), 3.85 (s, 2H), 3.74 – 3.65 (m, 4h), 3.52 (s, 2H), 2.75 (t, *J* = 7.0 Hz, 2H), 2.70 (s, 2H), 1.39 (s, 9H). ^{13}C NMR (101 MHz, DMSO-d_6) δ 169.16, 161.24, 158.93, 154.51, 154.28, 141.84, 137.86, 136.90, 135.94, 130.53, 129.18, 129.08 (2C), 121.87 (2C), 118.22, 115.29, 113.21, 95.38, 66.09 (2C), 57.29, 53.19 (2C), 45.23, 41.83, 38.82, 31.81, 30.30 (3C). LC-MS (ESI) *m/z*: [M + H]$^+$ 600.4. HPLC purity: 100%, t_R = 6.00 min. HRMS (ESI) *m/z*: [M + H]$^+$ calcd for $C_{31}H_{38}N_9O_2S$ 600.2869; found 600.2854.

*N-(2,3-dihydrobenzo[b][1,4]dioxin-6-yl)-2-(4-((6-(1-methyl-1H-pyrazol-4-yl)thieno[3,2-d]pyrimidin-4-yl)amino)phenyl)acetamide (**4f**).* The title compound was synthesized from **14** and 2,3-dihydrobenzo[*b*][1,4]dioxin-6-amine following general procedure A. White solid (69%). ^{1}H NMR (400 MHz, DMSO-d_6) δ 9.98 (s, 1H), 9.58 (s, 1H), 8.51 (s, 1H), 8.28 (s, 1H), 7.96 (s, 1H), 7.68 (d, *J* = 8.2 Hz, 2H), 7.53 (s, 1H), 7.30 (d, *J* = 8.2 Hz, 2H), 7.25 (d, *J* = 1.8 Hz, 1H), 6.98 (dd, *J* = 8.7, 1.8 Hz, 1H), 6.77 (d, *J* = 8.7 Hz, 1H), 4.19 (dd, *J* = 8.9, 4.5 Hz, 4h), 3.91 (s, 3H), 3.58 (s, 2H). ^{13}C NMR (101 MHz, DMSO-d_6) δ 168.75, 161.19, 154.59, 154.30, 142.87, 141.83, 139.22, 137.60, 136.90, 132.94, 131.16, 129.16, 129.11 (2C), 122.12 (2C), 118.20, 116.71, 115.30, 113.15, 112.33, 108.23, 64.16, 63.89, 42.73, 38.82. LC-MS (ESI) *m/z*: [M + H]$^+$ 499.2.

HPLC purity: 100%, t_R = 6.17 min. HRMS (ESI) *m/z*: $[M + H]^+$ calcd for $C_{26}H_{23}N_6O_3S$ 499.1552; found 499.1551.

*N-(4-(tert-butyl)phenyl)-2-(4-((6-(1-methyl-1H-pyrazol-4-yl)thieno[3,2-d]pyrimidin-4-yl)amino)phenyl)acetamide (**4g**).* The title compound was synthesized from **14** and 4-(*tert*-butyl)aniline following general procedure A. White solid (73%). ^{1}H NMR (400 MHz, DMSO-d_6) δ 10.08 (s, 1H), 9.59 (s, 1H), 8.51 (s, 1H), 8.28 (s, 1H), 7.95 (s, 1H), 7.69 (d, *J* = 7.9 Hz, 2H), 7.56 – 7.48 (m, 3H), 7.32 (d, *J* = 5.8 Hz, 2H), 7.30 (d, *J* = 5.9 Hz, 2H), 3.91 (s, 3H), 3.61 (s, 2H), 1.25 (s, 9H). ^{13}C NMR (101 MHz, DMSO-d_6) δ 169.00, 161.13, 154.59, 154.27, 145.47, 141.85, 137.59, 136.89, 136.66, 131.21, 129.17, 129.10 (2C), 125.26 (2C), 122.13 (2C), 118.91 (2C), 118.17, 115.30, 113.15, 42.76, 38.82, 33.96, 31.17 (3C). LC-MS (ESI) *m/z*: $[M + H]^+$ 497.2. HPLC purity: 99.1%, t_R = 7.35 min. HRMS (ESI) *m/z*: $[M + H]^+$ calcd for $C_{28}H_{29}N_6OS$ 497.2124; found 497.2100.

*N-(3-chloro-4-fluorophenyl)-2-(4-((6-(1-methyl-1H-pyrazol-4-yl)thieno[3,2-d]pyrimidin-4-yl)amino)phenyl)acetamide (**4h**).* The title compound was synthesized from **14** and 3-chloro-4-fluoroaniline following general procedure A. Beige solid (70%). ^{1}H NMR (400 MHz, DMSO-d_6) δ 10.37 (s, 1H), 9.59 (s, 1H), 8.51 (s, 1H), 8.29 (s, 1H), 7.98 – 7.92 (m, 2H), 7.70 (d, *J* = 8.4 Hz, 2H), 7.54 (s, 1H), 7.52 – 7.46 (m, 1H), 7.37 (t, *J* = 9.1 Hz, 1H), 7.31 (d, *J* = 8.4 Hz, 2H), 3.91 (s, 3H), 3.63 (s, 2H). ^{13}C NMR (101 MHz, DMSO-d_6) δ 169.52, 161.23, 154.55, 154.30, 152.99 (*J* = 243 Hz), 141.83, 137.76, 136.90, 136.45 (*J* = 3 Hz), 130.58, 129.17 (2C), 122.07 (2C), 120.45, 119.36 (*J* = 7 Hz), 119.07 (*J* = 18 Hz), 118.22, 116.92 (*J* = 21 Hz), 115.29, 113.17, 42.68, 38.83. LC-MS (ESI) *m/z*: $[M + H]^+$ 493.1. HPLC purity: 98.8%, t_R = 6.91 min. HRMS (ESI^+) *m/z*: $[M + H]^+$ calcd for $C_{24}H_{19}ClFN_6OS$ 493.1014; found 493.0999.

*N-(3-fluorobenzyl)-2-(4-((6-(1-methyl-1H-pyrazol-4-yl)thieno[3,2-d]pyrimidin-4-yl)amino)phenyl)acetamide (**4i**).* The title compound was synthesized from **14** and (3-fluorophenyl)methanamine following general procedure A. Yellow solid (58%). ^{1}H NMR (400 MHz, DMSO-d_6) δ 9.57 (s, 1H), 8.57 (t, *J* = 5.8 Hz, 1H), 8.51 (s, 1H), 8.28 (s, 1H), 7.96 (s, 1H), 7.67 (d, *J* = 8.1 Hz, 2H), 7.54 (s, 1H), 7.35 (d, *J* = 6.4 Hz, 1H), 7.27 (d, *J* = 8.2 Hz, 2H), 7.11 – 7.01 (m, 3H), 4.30 (d, *J* = 5.9 Hz, 2H), 3.91 (s, 3H), 3.49 (s, 2H). ^{13}C NMR (101 MHz, DMSO-d_6) δ 170.41, 161.22, 162.18 (*J* = 243 Hz), 154.58, 154.31, 142.57 (*J* = 8 Hz), 141.81, 137.53, 136.89, 131.38, 130.18 (*J* = 8 Hz), 129.17, 129.05 (2C), 123.10 (*J* = 2 Hz), 122.04 (2C), 118.21, 115.29, 113.76 (*J* = 21 Hz), 113.46 (*J* = 21 Hz), 113.13, 41.81, 41.70, 38.82. LC-MS (ESI) *m/z*: $[M + H]^+$ 473.1. HPLC purity: 98.5%, t_R = 6.19 min. HRMS (ESI) *m/z*: $[M + H]^+$ calcd for $C_{25}H_{22}FN_6OS$ 473.1560; found 473.1550.

*2-(4-((6-(1-methyl-1H-pyrazol-4-yl)thieno[3,2-d]pyrimidin-4-yl)amino)phenyl)-N-(pyridin-3-yl)acetamide (**4**).* The title compound was synthesized from **14** and pyridin-3-amine following general procedure A. Yellow solid (66%). ^{1}H NMR (400 MHz, DMSO-d_6) δ 10.39 (s, 1H), 9.60 (s, 1H), 8.76 (s, 1H), 8.51 (s, 1H), 8.29 (s, 1H), 8.26 (d, *J* = 4.5 Hz, 1H), 8.05 (d, *J* = 8.4 Hz, 1H), 7.96 (s, 1H), 7.70 (d, *J* = 8.3 Hz, 2H), 7.54 (s, 1H), 7.34 (t, *J* = 8.7 Hz, 3H), 3.91 (s, 3H), 3.67 (s, 2H). ^{13}C NMR (101 MHz, DMSO-d_6) δ 169.84, 161.22, 154.57, 154.30, 144.14, 141.83, 140.75, 137.74, 136.90, 130.64, 129.21 (2C), 129.16, 126.03, 123.61, 122.11(2C), 118.21, 115.30, 113.17, 42.58, 38.82. LC-MS (ESI) *m/z*: $[M + H]^+$ 442.3. HPLC purity: 99.7%, t_R = 4.94 min. HRMS (ESI) *m/z*: $[M + H]^+$ calcd for $C_{23}H_{20}N_7OS$ 442.1450; found 442.1440.

*2-(4-((6-bromothieno[3,2-d]pyrimidin-4-yl)amino)phenyl)-N-(4-chloro-3-fluorophenyl)acetamide (**16**).* The title compound was synthesized from **15** and 3-chloro-4-fluoroaniline following general procedure A. Yellow solid (88%). ^{1}H NMR (400 MHz, DMSO-d_6) δ 10.40 (s, 1H), 9.76 (s, 1H), 8.51 (s, 1H), 7.94 (dd, *J* = 6.9, 2.5 Hz, 1H), 7.67 (s, 1H), 7.65 (d, *J* = 8.4 Hz, 2H), 7.51 – 7.46 (m, 1H), 7.37 (t, *J* = 9.1 Hz, 1H), 7.33 (d, *J* = 8.4 Hz, 2H), 3.64 (s, 2H). LC-MS (ESI) *m/z*: $[M + H]^+$ 491.2/493.2.

General procedure B: *Synthesis of compounds **2**, **10**, **13**, and **18***. Chloride **5**, or **12** (0.2 mmol), amine **8**, **9**, or **17** (0.2 mmol) were suspended in isopropanol (4 mL). The reaction mixture was irradiated under microwave at 100 °C for 0.5 h. The completion of the reaction was monitored by LC-MS analysis. The reaction mixture was filtered to get the titled compound.

*N-(4-methoxyphenyl)thieno[3,2-d]pyrimidin-4-amine (**2a**)*. The title compound was synthesized from **5** and 4-methoxyaniline following general procedure B. Yellow solid (92%). ^{1}H NMR (400 MHz, DMSO-d_6) δ 11.46 (s, 1H), 8.87 (s, 1H), 8.47 (d, *J* = 5.3 Hz, 1H), 7.58 (d, *J* = 5.4 Hz, 1H), 7.54 (d, *J* = 8.6 Hz, 2H), 7.04 (d, *J* = 8.8 Hz, 2H) , 3.80 (s, 3H). ^{13}C NMR (101 MHz, DMSO-d_6) δ 168.62, 157.13, 148.83, 147.83, 140.02, 128.85, 126.93, 118.21 (2C), 114.18 (2C), 55.41. LC-MS (ESI) *m/z*: $[M + H]^+$ 258.1. HPLC purity 99.8%, t_R = 6.93 min.

*N-(4-fluorophenyl)thieno[3,2-d]pyrimidin-4-amine (**2b**)***.*** The title compound was synthesized from **5** and 4-fluoroaniline following general procedure B. Beige solid (88%). ^{1}H NMR (400 MHz, DMSO-d_6) δ 11.38 (s, 1H), 8.89 (s, 1H), 8.50 (d, *J* = 5.4 Hz, 1H), 7.74 – 7.68 (m, 2H), 7.59 (d, *J* = 5.5 Hz, 1H), 7.36 – 7.29 (m, 2H). ^{13}C NMR (101 MHz, DMSO-d_6) δ 160.17 (*J* = 248 Hz), 158.94, 156.75, 149.49, 145.77, 139.59, 133.03, 126.80 (*J* = 12 Hz, 2C), 119.00, 115.67 (*J* = 23 Hz, 2C). LC-MS (ESI) *m/z*: $[M + H]^+$ 246.0. HPLC purity 97.1%, t_R = 7.88 min.

*piperidin-1-yl(4-(thieno[3,2-d]pyrimidin-4-ylamino)phenyl)methanone (**2c**).* The title compound was synthesized from **5** and (4-aminophenyl)(piperidin-1-yl)methanone following general procedure B. Yellow solid (85%). ^{1}H NMR (400 MHz, DMSO-d_6) δ 11.57 (s, 1H), 8.93 (s, 1H), 8.55 (d, *J* = 5.4 Hz, 1H), 7.81 (d, *J* = 8.3 Hz, 2H), 7.63 (d, *J* = 5.4 Hz, 1H), 7.46 (d, *J* = 8.3 Hz, 2H), 3.56 - 3.35 (m, 4H), 1.68 – 1.42 (m, 6H). ^{13}C NMR (101 MHz, DMSO-d_6) δ 168.33, 156.41, 149.38, 139.76, 137.80, 133.76, 127.39 (2C), 123.65, 118.99 (2C), 116.30, 109.55, 48.14 (2C), 25.52 (2C), 24.05. LC-MS (ESI) *m/z*: $[M + H]^+$ 339.1. HPLC purity 99.5%, t_R = 7.43 min.

*ethyl 2-(4-(thieno[3,2-d]pyrimidin-4-ylamino)phenyl)acetate (**10**).* The title compound was synthesized from **5** and **9** following general procedure B. Beige solid (91%). ^{1}H NMR (400 MHz, DMSO-d_6) δ 11.33 (s, 1H), 8.87 (s, 1H), 8.50 (d, *J* = 5.3 Hz, 1H), 7.61 (d, *J* = 8.1 Hz, 2H), 7.58 (d, *J* = 5.4 Hz, 1H), 7.36 (d, *J* = 8.1 Hz, 2H), 4.09 (q, *J* = 7.1 Hz, 2H), 3.71 (s, 2H), 1.20 (t, *J* = 7.1 Hz, 3H). LC-MS (ESI) *m/z*: $[M + H]^+$ 314.3.

*ethyl 2-(4-((6-bromothieno[3,2-d]pyrimidin-4-yl)amino)phenyl)acetate (**13**).* The title compound was synthesized from **12** and **9** following general procedure B. Beige solid (87%). ^{1}H NMR (400 MHz, DMSO-d_6) δ 10.84 (s, 1H), 8.73 (s, 1H), 7.73 (s, 1H), 7.61 (d, *J* = 8.2 Hz, 2H), 7.33 (d, *J* = 8.3 Hz, 2H), 4.09 (q, *J* = 7.3 Hz, 2H), 3.70 (s, 2H), 1.19 (t, *J* = 7.3 Hz, 3H). LC-MS (ESI) *m/z*: $[M + H]^+$ 392.1/394.3.

*tert-butyl (4-((6-bromothieno[3,2-d]pyrimidin-4-yl)amino)phenyl)carbamate (**18**).* The title compound was synthesized from **12** and **18** following general procedure B. Beige solid (93%). ^{1}H NMR (400 MHz, DMSO-d_6) δ 10.97 (s, 1H), 9.53 (s, 1H), 8.74 (s, 1H), 7.72 (d, *J* = 1.5 Hz, 1H), 7.54 (d, *J* = 9.0 Hz, 2H), 7.49 (d, *J* = 8.9 Hz, 2H), 1.49 (s, 9H). LC-MS (ESI) *m/z*: $[M + H]^+$ 421.3/423.3.

Synthesis of compound 4k.

Step 1. **18** (0.3 mmol), 1-methyl-4-(4,4,5,5-tetramethyl-1,3,2-dioxaborolan-2-yl)-1*H*-pyrazole (0.5 mmol), and $NaHCO_3$ (1.2 mmol) were dissolved in THF (2 mL) and H_2O (2 mL). The solution was degassed for 5 min, then $Pd(PPh_3)_4$ (0.03 mmol) was added. The reaction mixture was irradiated under microwave at 140 °C for 0.5 h. The consumption of starting materials was detected by LC-MS analysis. The reaction mixture was concentrated in vacuum. The resulting residue was purified by silica gel chromatography to get yellow solid (120 mg, yield 86%). ^{1}H NMR (400 MHz, $CDCl_3$) δ 8.56 (s, 1H), 7.70 (d, *J* = 8.4 Hz, 2H), 7.52 – 7.45 (m, 3H), 7.42 (d, *J* = 8.4 Hz, 2H), 6.64 (s, 1H), 3.94 (s, 3H), 1.55 (s, 9H). LC-MS (ESI) *m/z*: $[M + H]^+$ 423.2. The solid was dissolved in DCM (2 mL) and TFA (1 mL) was added. The mixture was stirred at ambient temperature

overnight. The completion of the reaction was monitored by LC-MS analysis. The reaction mixture was concentrated in vacuum. The resulting residue was dissolved in DCM (100 mL) and washed with saturated $NaHCO_3$ solution, water and brine twice. The organic phase was concentrated in vacuum to get **19** as a yellow solid (85 mg, 93%). ^{1}H NMR (400 MHz, $CDCl_3$) δ 8.55 (s, 1H), 7.70 (s, 1H), 7.63 (s, 1H), 7.30 (s, 1H), 7.22 (d, *J* = 8.6 Hz, 2H), 6.74 (d, *J* = 8.7 Hz, 2H), 3.93 (s, 3H). LC-MS (ESI) *m/z*: $[M + H]^+$ 323.1.

Step 2. 3-(*tert*-butyl)-1-methyl-1*H*-pyrazol-5-amine (0.06 mmol) and triphogene (0.03 mmol) was dissolved in DCM (1 mL). A solution of Et_3N in DCM (0.15 mmol Et_3N in 1 mL DCM) was added slowly at 0 °C. The reaction mixture was warmed to ambient temperature and stirred for 2 h. The reaction mixture was added slowly into a solution of **19** (0.05 mmol) in DCM (1 mL) at ambient temperature. The resulting reaction mixture was stirred at ambient temperature for 5 h. The completion of the reaction was monitored by LC-MS analysis. The reaction mixture was poured into water and extracted with DCM. The organic phase was washed with water and brine twice, and concentrated in vacuum. The resulting residue was purified by silica gel chromatography to get **4k** as a yellow solid (20 mg, 66%). ^{1}H NMR (400 MHz, $CDCl_3$) δ 8.45 (s, 1H), 7.78 (s, 1H), 7.70 (s, 1H), 7.49 (d, *J* = 8.8 Hz, 2H), 7.36 (d, *J* = 8.8 Hz, 2H), 7.32 (s, 1H), 6.22 (s, 1H), 3.89 (s, 3H), 3.71 (s, 3H), 1.25 (s, 9H). LC-MS (ESI) *m/z*: $[M + H]^+$ 502.0. HPLC purity: 97.2%, t_R = 7.90 min. HRMS (ESI) *m/z*: $[M + H]^+$ calcd for $C_{25}H_{28}N_9OS$ 502.2138; found 502.2128.

General procedure C: *Synthesis of compounds **4l-n***. **16** (0.1 mmol), boronic acid (0.15 mmol), and $NaHCO_3$ (0.3 mmol) were dissolved in THF (2mL) and H_2O (2mL). The solution was degassed for 5 min, then $Pd(PPh_3)_4$ (0.005 mmol) was added. The reaction mixture was irradiated under microwave at 140 °C for 0.5 h. The consumption of starting materials was detected by LC-MS analysis. The reaction mixture was poured into water and extracted with ethyl acetate. The organic phase was washed with water and brine twice, and concentrated in vacuum. The resulting residue was purified by silica gel chromatography to get the title compound.

*N-(3-chloro-4-fluorophenyl)-2-(4-((6-(4-(methylsulfonyl)phenyl)thieno[3,2-d]pyrimidin-4-yl)amino)phenyl)acetamide (**4l**)*. The title compound was synthesized from **16** and (4-(methylsulfonyl)phenyl)boronic acid following general procedure C. Yellow solid (66%). ^{1}H NMR (400 MHz, DMSO-d_6) δ 10.39 (s, 1H), 9.83 (s, 1H), 8.59 (s, 1H), 8.17 – 8.10 (m, 3H), 8.06 (d, *J* = 8.5 Hz, 2H), 7.94 (dd, *J* = 6.8, 2.5 Hz, 1H), 7.73 (d, *J* = 8.5 Hz, 2H), 7.52 – 7.47 (m, 1H), 7.40 – 7.31 (m, 3H), 3.65 (s, 2H), 3.29 (s, 3H).

^{13}C NMR (101 MHz, DMSO-d_6) δ 169.49, 160.76, 154.91, 154.69, 152.99 (J = 243 Hz), 147.08, 141.19, 137.49, 137.32, 136.45 (J = 3 Hz), 130.99, 129.26 (2C), 128.09 (2C), 127.07 (2C), 122.88, 122.32 (2C), 120.45, 119.36 (J = 6 Hz), 119.09 (J = 18 Hz), 116.92 (J = 21 Hz), 115.80, 43.42, 42.68. LC-MS (ESI) *m/z*: $[M + H]^+$ 567.3. HPLC purity 95.0%, t_R = 7.06 min.

*N-(3-chloro-4-fluorophenyl)-2-(4-((6-(3,4,5-trimethoxyphenyl)thieno[3,2-d]pyrimidin-4-yl)amino)phenyl)acetamide (**4m**).* The title compound was synthesized from **16** and (3,4,5-trimethoxyphenyl)boronic acid following general procedure C. Beige solid (62%). ^{1}H NMR (400 MHz, DMSO-d_6) δ 10.37 (s, 1H), 9.68 (s, 1H), 8.57 (s, 1H), 7.96 – 7.92 (m, 2H), 7.75 (d, J = 8.6 Hz, 2H), 7.51 – 7.46 (m, 1H), 7.38 (d, J = 9.1 Hz, 1H), 7.35 – 7.30 (m, 2H), 7.14 (s, 2H), 3.90 (s, 6H), 3.73 (s, 3H), 3.64 (s, 2H). ^{13}C NMR (101 MHz, DMSO-d_6) δ 169.52, 161.04, 154.60, 154.46, 153.40 (2C), 152.99 (J = 243 Hz), 149.59, 138.76, 137.77, 136.45 (J = 3 Hz), 130.58, 129.21 (2C), 128.24, 121.88 (2C), 120.48, 120.45, 119.36 (J = 7 Hz), 119.07 (J = 18 Hz), 116.92 (J = 21 Hz), 114.67, 103.81 (2C), 60.17, 56.09 (2C), 42.67. LC-MS (ESI) *m/z*: $[M + H]^+$ 579.1. HPLC purity 98.0%, t_R = 7.49 min.

*N-(3-chloro-4-fluorophenyl)-2-(4-((6-(4-(2-(pyrrolidin-1-yl)ethoxy)phenyl)thieno[3,2-d]pyrimidin-4-yl)amino)phenyl)acetamide (**4n**)*. The title compound was synthesized from **16** and (4-(2-(pyrrolidin-1-yl)ethoxy)phenyl)boronic acid following general procedure C. Yellow solid (52%). ^{1}H NMR (400 MHz, DMSO-d_6) δ 10.35 (s, 1H), 9.61 (s, 1H), 8.49 (s, 1H), 7.91 (dd, J = 6.9, 2.5 Hz, 1H), 7.75 (d, J = 8.7 Hz, 2H), 7.72 (s, 1H), 7.67 (d, J = 8.4 Hz, 2H), 7.48 – 7.42 (m, 1H), 7.33 (t, J = 9.1 Hz, 1H), 7.28 (d, J = 8.4 Hz, 2H), 7.04 (d, J = 8.8 Hz, 2H), 4.10 (t, J = 5.8 Hz, 2H), 3.60 (s, 2H), 2.78 (t, J = 5.8 Hz, 2H), 2.48 – 2.44 (m, 3H), 1.69 – 1.61 (m, 4H). ^{13}C NMR (101 MHz, DMSO-d_6) δ 169.54, 161.34, 159.71, 154.66, 154.39, 153.01 (J = 243 Hz), 149.59, 137.71, 136.47 (J = 3 Hz), 130.73, 129.21 (2C), 127.74 (2C), 125.13, 122.22 (2C), 120.47, 119.36 (J = 7 Hz), 119.08 (J = 18 Hz), 118.92, 116.93 (J = 22 Hz), 115.29 (2C), 114.16, 66.96, 54.18, 53.98 (2C), 42.70, 23.15 (2C). LC-MS (ESI) *m/z*: $[M + H]^+$ 602.2. HPLC purity 98.1%, t_R = 6.34 min.

General procedure D: *Synthesis of acids **7** and **14***. Chloride **5** or bromide **13** (3.5 mmol), boronic ester (3.5 mmol), and $NaHCO_3$ (14 .0 mmol) were dissolved in THF (5mL) and H_2O (5mL). The solution was degassed for 5 min, then $Pd(PPh_3)_4$ (0.2 mmol) was added. The reaction mixture was irradiated under microwave at 140 °C for 0.5 h. The consumption of starting materials was detected by LC-MS analysis. LiOH (14.0 mmol) was added and the reaction mixture was irradiated under microwave at 100 °C for 0.5 h. The consumption of starting materials was detected by LC-MS analysis. The resulting mixture was adjusted to pH 3-4 with 1 N HCl aq solution. The resulting suspension was stirred for 5 h then filtered. The residue was dried under vacuum at 45 °C overnight to get the titled compound.

*2-(4-(thieno[3,2-d]pyrimidin-4-yl)phenyl)acetic acid (**7**).* The title compound was synthesized from **5** and **6** following general procedure D. Grey solid (yield, 82%) ^{1}H NMR (400 MHz, DMSO-d_6) δ 9.26 (s, 1H), 8.57 (d, *J* = 5.5 Hz, 1H), 8.14 (d, *J* = 8.2 Hz, 2H), 7.73 (d, *J* = 5.5 Hz, 1H), 7.55 (d, *J* = 8.0 Hz, 2H), 3.73 (s, 2H). LC-MS (ESI) *m/z*: $[M + H]^+$ 271.0.

*2-(4-((6-(1-methyl-1H-pyrazol-4-yl)thieno[3,2-d]pyrimidin-4-yl)amino)phenyl)acetic acid (**14**)*. The title compound was synthesized from **13** and 1-methyl-4-(4,4,5,5-tetramethyl-1,3,2-dioxaborolan-2-yl)-1*H*-pyrazole following general procedure D. Grey solid (yield, 77%) ^{1}H NMR (400 MHz, DMSO-d_6) δ 12.32 (s, 1H), 9.58 (s, 1H), 8.51 (s, 1H), 8.29 (s, 1H), 7.96 (s, 1H), 7.68 (d, *J* = 8.4 Hz, 2H), 7.54 (s, 1H), 7.24 (d, *J* = 8.4 Hz, 2H), 3.91 (s, 3H), 3.55 (s, 2H). LC-MS (ESI) *m/z*: $[M + H]^+$ 366.1.

Synthesis of compound 11. A mixture of **10** (4.0 mmol) and LiOH (16.0 mmol) in THF (5 mL) and H_2O (5 mL) was irradiated under microwave at 100 °C for 0.5 h. The consumption of starting materials was detected by LC-MS analysis. The resulting mixture was adjusted to pH 3-4 with 1 N HCl solution. The resulting suspension was stirred for 5 h then filtered. The residue was dried under vacuum at 45 °C overnight to get the titled compound (980 mg, yield 86%). ^{1}H NMR (400 MHz, DMSO-d_6) δ 12.31 (s, 1H), 9.68 (s, 1H), 8.56 (s, 1H), 8.22 (d, *J* = 5.2 Hz, 1H), 7.70 (d, *J* = 7.9 Hz, 2H), 7.46 (d, *J* = 5.4 Hz, 1H), 7.25 (d, *J* = 8.0 Hz, 2H), 3.56 (s, 2H). LC-MS (ESI) *m/z*: $[M + H]^+$ 286.3.

Synthesis of compound 24.

Step 1. 2-(5-amino-3-(*tert*-butyl)-1*H*-pyrazol-1-yl)ethanol[34] (27.3 mmol) and Et_3N (81.8 mmol) was dissolved in DCM (100 mL). A solution of TsCl (81.8 mmol) in DCM (100 mL) was added dropwise. The resulting reaction

mixture was refluxed overnight. The consumption of starting materials was detected by LC-MS analysis. Water (100 mL) was added into the reaction mixture. Separate the organic phase and concentrated in vacuum. The resulting residue was purified by silica gel chromatography to get **21** as a beige solid (8.8 g, yield 50%). ^{1}H NMR (400 MHz, $CDCl_3$) δ 7.77 (dd, *J* = 11.5, 8.3 Hz, 6H), 7.36 (d, *J* = 8.1 Hz, 4h), 7.30 (d, *J* = 8.1 Hz, 2H), 5.66 (s, 1H), 4.35 (t, *J* = 6.4 Hz, 2H), 3.91 (t, *J* = 6.4 Hz, 2H), 2.49 (s, 6H), 2.42 (s, 3H). LC-MS (ESI) *m/z*: $[M + H]^+$ 646.2.

Step 2. A mixture of **21** (3.0 mmol) in morpholine (30 mL) was heated to 120 °C overnight. The consumption of starting materials was detected by LC-MS analysis. Water (100 mL) and DCM (200 mL) was added into the reaction mixture. The organic phase was washed with water and brine twice, and concentrated in vacuum. The resulting residue was purified by silica gel chromatography to get **22** as colorless oil (0.8 g, yield 64%). ^{1}H NMR (400 MHz, $CDCl_3$) δ 7.63 (d, *J* = 8.1 Hz, 2H), 7.23 (d, *J* = 8.1 Hz, 2H), 5.99 (s, 1H), 3.91 (t, *J* = 4.6 Hz, 4h), 3.88 – 3.83 (m, 2H), 2.68 – 2.62 (m, 2H), 2.58 (s, 4h), 2.39 (s, 3H), 1.22 (s, 9H). LC-MS (ESI) *m/z*: 646.2 $[M + H]^+$. Also get **23** as colorless oil (0.36 g, yield 30%). ^{1}H NMR (400 MHz, $CDCl_3$) δ 7.68 (d, *J* = 7.9 Hz, 2H), 7.26 (d, *J* = 8.1 Hz, 2H), 5.91 (s, 1H), 4.11 (t, *J* = 7.6 Hz, 2H), 3.97 (t, *J* = 7.5 Hz, 2H), 2.39 (s, 3H), 1.26 (s, 9H). LC-MS (ESI) *m/z*: $[M + H]^+$ 320.1.

Step 3. A mixture of **22** (0.9 mmol) in H_2SO_4 was stirred at ambient temperature overnight. The consumption of starting materials was detected by LC-MS analysis. The reaction mixture was poured into iced water and adjusted to pH 8-9 with 2N NaOHaq solution. The resulting mixture was concentrated in vacuum to get crude **24** as a white solid. LC-MS (ESI) *m/z*: $[M + H]^+$ 253.1.

Enzymatic assay:

TRKA-C activity was measured via a mobility shift assay monitoring the separation of the phosphorylated product from substrate. In 96-well plates, compound stock solution (20 mM in DMSO) were diluted with kinase buffer (10 mM HEPES, 0.05% Triton X-100, 5% glycerol, 5 mM DTT, 10 mM $MgCl_2$, 10 mM $MnCl_2$ and 0.1 mg/mL BSA) in 12-point ½log dilutions (2 mM–6.32 nM). The TRKA enzyme (Life Technologies, CA, USA) was diluted to 2.35 µg/ml with the kinase buffer. Then, 4 µl of the TRKA solution and 1 µl of the diluted compound solution were transferred to a 384-well assay plate to be incubated for 1 hour. 1 µl of kinase buffer was added in the positive control instead of the compound solution and 5 µl of the kinase buffer were added to the negative control.

After the pre-incubation, 5 µl of the substrate mix containing 10 µM ATP and 3 µM 5-FAM tagged peptide (peptide substrate #22, 5-FAM-EEPLYWSFPAKKK-$CONH_2$ [PerkinElmer, MA, USA]) in kinase buffer were added to the assay plate. Final running concentrations were as follows: ATP (5 µM), peptide (1.5 µM), compounds (0.2 mM–0.632 nM). Entrectinib was used as the running control. The plate was run on the Caliper EZ Reader II (PerkinElmer, MA, USA) with separation buffer (100 mM HEPES, 10 mM EDTA, 0.015% Brij-35, 0.1% CR-3 [PerkinElmer, MA, USA]) until 10–20% conversion based on the positive control wells. The following separation conditions were utilized: upstream voltage −500V; downstream voltage, −1900V; chip pressure −0.8. Dose-response curves were generated in GraphPad Prisim 8 and IC_{50} values were obtained from the curves. IC_{50} values were generated in duplicate and error was calculated from the standard deviation between two values.

Cellular assay:

KM12 cells were cultured using RPMI-1640 (Gibco, CA, USA) growth medium containing 10% fetal bovine serum (FBS) (Gibco, Carlsbad, USA), 100 U/ml penicillin (Gibco, Carlsbad, USA) and 100 U/ml streptomycin (Gibco, CA, USA). The cells were cultured at 37°C in a humidified atmosphere with 5% CO_2. To do the viability assay, cells were seeded in 96-well cell culture plates. After 24-hour incubation, cells were exposed to 7 concentrations of compounds ranging from 200 to 0.0002 µM for 72 hours. Meantime, DMSO were added to the controls. Resazurin staining viability assay (Biotium, CA, USA) was used to determine the cell viability at the end of compound treatment. Then, IC_{50} values were calculated from the dose-response curves which were generated in GraphPad Prism 8. Error was determined as the standard deviation between two independent IC_{50} measurements.

Western blot:

Cells were harvested in lysis buffer (50 mM Hepes, pH 7.5, 150 mM NaCl, 10% glycerol, 1% Triton X-100, 1 mM EGTA, 1.5 mM $MgCl_2$, 10 mM NaF, 10 mM sodium pyrophosphate, 1 mM Na_3VO_4, 10 µg of aprotinin/ml, 10 µg of leupeptin/ml) and clarified by centrifugation at 10,000 x *g*. Protein concentration was estimated with a modified Bradford assay (Bio-Rad, Munich, Germany). Antigens were revealed by an enhanced chemiluminescence detection kit (Pierce ECL, ThermoFisher Scientific, Waltham, MA, USA) [14]. Phospho-TRKA (Tyr490) (#9141), and phospho-TRKA (Tyr674/675) (#4621) antibodies were from Cell Signaling Technology (Danvers, MA, USA). Anti-TRKA (C-14) (#sc-11) antibody was from Santa Cruz Biotechnology

(Santa Cruz, CA, USA). Anti phospho-tyrosine, clone 4G10 (05-321) antibody was from Merck Millipore (Billerica, MA, USA). Secondary antibodies coupled to horseradish peroxidase were purchased from Bio-Rad.

Molecular modeling:

Molecular modeling studies were performed using AutoDock Tools, AutoDock Vina,[35] and Maestro 2018-2. TRKA crystal structure (PDB ID: 6PL1) was retrieved from RCSB Protein Data Bank. Using AutoDock Tools, the TRK model was prepared as follows: (i) remove all waters; (ii) add all hydrogen as 'Polar Only'; (iii) generate a grid box for the ATP binding site, which includes the hinge region, DFG residues and the residues of the αC-helix facing the ATP pocket. Compounds to be docked were assigned torsions around rotatable bonds using AutoDock Tools and were docked into the grid by using Autodock Vina. The docking results were visualized and analyzed with Maestro 2018-2.

***In vitro* human brain-like endothelial cells (BLEC) BBB model:**

A human BBB model was then used in order to predict entrectinib and **4c** passage. The human *in vitro* BBB model derived from hematopoietic stem cells was prepared as described previously.[36] Infants' parents signed a consent form and cells were manipulated following the procedure validated by the local ethical committee and French ministry of Research. Briefly, CD34+ cells were isolated from human umbilical cord blood by ficoll density gradient and using the mini-MACS immunomagnetic separation system (Miltenyi Biotec, Bergisch Gladbach), according to the manufacturer's recommendations. These CD34 positive cells were subsequently were transferred onto 1% (w/v) gelatin coated 24-well plates (2 x 10^5 cells/well) and incubated in endothelial growth medium (EGM-2; Lonza, Gaithersburg, MD, USA) with 20% (v/v) fetal bovine serum (FBS; Invitrogen,Carlsbad, USA) and 50 ng/mL vascular endothelial growth factor (VEGF165; PrepoTech Inc., Rocky Hill, USA), at 5% CO_2, 37°C. After 2-3 weeks they are differentiated into endothelial cells and endothelial markers are checked by western blot, FACs and quantitative PCR.[37] Then, CD34+derived endothelial cells were co-cultivated with bovine brain pericytes in Transwell™ Costar polycarbonate inserts, 0.4 µm pore size, coated with matrigel® (Corning) in a complete medium (ScienCell). Brain péricytes were isolated as previously described.[38] After 6 days of co-culture, CD34+-derived endothelial cells have acquired BBB properties induced by brain pericytes as previously described.[39] This model is then named Human brain like-endothelial cells (BLECs) and is routinely used to determine molecules toxicity and delivery into the CNS.[40-42]

Endothelial permeability measurement

Endothelial permeability coefficients were determined as described by Dehouck et al.[43] The inserts, containing an endothelial cell monolayer or only coated with matrigel, were transferred into 12-well plates containing 1.5 mL of Ringer-HEPES (RH) bufferer saline (150 mM NaCl, 5.2 mM KCl, 2.2 mM $CaCl_2$, 0.2 mM $MgCl_2$, 0.6 mM $NaHCO_3$, 5 mM HEPES, pH 7.4) per well, thus constituting the abluminal compartment. Then, 0.5 mL of RH buffer saline containing 10 µM of the compound to be tested (entrectinib or **4c**) was added to the upper (luminal) compartment, in place of the culture medium in contact with the BLECs. After different time-points (30, 60, and 120 min), filters were transferred into a new well filled with RH buffer saline. All incubations were performed at 37 °C and stopped at 120 minutes.

To assess the toxicity of the molecules on the BLECs, Lucifer yellow (LY) (Sigma-Aldrich, L0259) that poorly crosses the BBB, was used as the monolayer integrity marker. Diffusion of 25 µM LY was tested alone (control) or incubated with entrectinib or **4c**, as described above. At 120 min, a 200 µL aliquot from a lower compartment at each time point and a 20 µL aliquot of the initial solution placed in the upper compartment were measured using a fluorimeter (Synergy H1; BioTek, Winooski, VT, USA) to calculate the LY concentration.

Concentrations of entrectinib or **4c** were determined by LC-MS (Waters ACQUITY UPLC System with ACQUITY QDa mass spectrometer) in the solutions from the upper and lower compartments. The endothelial permeability coefficients (Pe) to LY, entrectinib and **4c**, were calculated using the clearance principle to generate a concentration-independent parameter as described by Siflinger-Birnboim *et al*.[44] First, the volumes cleared were plotted versus time (30 and 60 min) and the slopes were estimated by linear regression for both insert only coated with matrigel (PSf) and for insert coated with matrigel and seeded with cells (PSt). PSe was calculated according to the following formula: 1/PSe = 1/PSt-1/PSf where "S" represented the surface area of the porous membrane of the insert. PSe was divided by the membrane surface (1.12 cm^2) to generate the endothelial Pe to the studied molecules expressed in cm/min.

To assess possible adsorption, aggregation and/or degradation of molecules during the transport experiments, their mass balances (recovery in %) were calculated at 120 min from the amount of compound recovered in both compartments at the end of the experiment divided by the total amount added in the donor compartment at the start of the experiment.

$$\text{M.B.(\%)} = \frac{\text{Drug amount recovered in media at the end of the experiment x 100}}{\text{Drug amount in the donor compartment at the onset of the experiment}}$$

Author Information

Corresponding Author

*H. L.: e-mail, HLi2@uams.edu

Author contributions

The idea was conceived by WY, BF and HL. The synthesis was done by WY and FL. The biological assays were performed by LZ, MM, FC and CL. The article was written by WY and edited by all.

†WY and LZ contributed equally.

Declaration of competing interest

The authors declare no competing financial interest.

Acknowledgments

The authors would like to thank Dr. Ryoichi Fujiwara, the director of UAMS Analytical and Bioanalytical Core (CORE B), for providing services for quantification of small molecules. This work was supported by NCI 1R01CA197178 (to HL) and the POR Campania FESR 2014-2020 “SATIN” grant (to MS and FC).

Appendix A. Supplementary data

The following is the Supplementary data to this article: ^{1}H NMR, ^{3}C NMR and HPLC spectra of final compounds. Supplementary information for endothelial permeability measurement assay.

References

[1] K.O. Lai, A.S. Wong, M.C. Cheung, P. Xu, Z. Liang, K.C. Lok, H. Xie, M.E. Palko, W.H. Yung, L. Tessarollo, Z.H. Cheung, N.Y. Ip, TrkB phosphorylation by Cdk5 is required for activity-dependent structural plasticity and spatial memory, *Nat Neurosci*, 15 (2012). 1506-1515. 10.1038/nn.3237.

[2] E. Huang, L.F. Reichardt, Trk receptors: roles in neuronal signal transduction, *Annu Rev Biochem*, 72 (2003). 6[illegible]-6[illegible]. 10.1146/annurev.biochem.72.121801.161629.

[3] W. Yan, N.R. Lakkaniga, F. Carlomagno, M. Santoro, N.Q. McDonald, F. Lv, N. Gunaganti, B. Frett, H.Y. Li, Insights into current tropomyosin receptor kinase (TRK) inhibitors: development and clinical application, *J Med Chem*, 62 (2019). 1731-1760. 10.1021/acs.jmedchem.8b01092.

[4] A. Amatu, A. Sartore-Bianchi, S. Siena, NTRK gene fusions as novel targets of cancer therapy across multiple tumour types, *ESMO Open*, 1 (2016). e000023. 10.1136/esmoopen-2015-000023.

[5] D. Martin-Zanca, S.H. Hughes, M. Barbacid, A human oncogene formed by the fusion of truncated tropomyosin and protein tyrosine kinase sequences, *Nature*, 319 (1986). 743-748. 10.1038/319743a0.

[6] D. Martin-Zanca, R. Oskam, G. Mitra, T. Copeland, M. Barbacid, Molecular and biochemical characterization of the human trk proto-oncogene, *Mol Cell Biol*, 9 (1989). 24-33. 10.1128/mcb.9.1.24.

[7] A. Vaishnavi, A.T. Le, R.C. Doebele, TRKing down an old oncogene in a new era of targeted therapy, *Cancer Discov*, 5 (2015). 25-34. 10.1158/2159-8290.CD-14-0765.

[8] M.J. Edel, A. Shvarts, J.P. Medema, R. Bernards, An in vivo functional genetic screen reveals a role for the TRK-T3 oncogene in tumor progression, *Oncogene*, 23 (2004). 4959-4965. 10.1038/sj.onc.1207667.

[9] https://www.fda.gov/drugs/fda-approves-larotrectinib-solid-tumors-ntrk-gene-fusions. Jul. 30th, 2020

[10]https://www.fda.gov/drugs/resources-information-approved-drugs/fda-approves-entrectinib-ntrk-solid-tumors-and-ros-1-nsclc. Jul. 30th, 2020

[11] A.C. Dar, K.M. Shokat, The evolution of protein kinase inhibitors from antagonists to agonists of cellular signaling, *Annu Rev Biochem*, 80 (2011). 769-795. 10.1146/annurev-biochem-090308-173656.

[12] M.P. Mattson, Glutamate and neurotrophic factors in neuronal plasticity and disease, *Ann N Y Acad Sci*, 1144 (2008). 97-112. 10.1196/annals.1418.005.

[13] E.E. Noble, C.J. Billington, C.M. Kotz, C. Wang, The lighter side of BDNF, *Am J Physiol Regul Integr Comp Physiol*, 300 (2011). R1053-R1069. 10.1152/ajpregu.00776.2010.

[14] E. Sanchez-Ortiz, D. Yui, D. Song, Y. Li, J.L. Rubenstein, L.F. Reichardt, L.F. Parada, TrkA gene ablation in basal forebrain results in dysfunction of the cholinergic circuitry, *J Neurosci*, 32 (2012). 4065-4079. 10.1523/JNEUROSCI.6314-11.2012.

[15] V. Nikoletopoulou, H. Lickert, J.M. Frade, C. Rencurel, P. Giallonardo, L. Zhang, M. Bibel, Y.A. Barde, Neurotrophin receptors TrkA and TrkC cause neuronal death whereas TrkB does not, *Nature*, 467 (2010). 59-63. 10.1038/nature09338.

[16] T. Wang, D. Yu, M.L. Lamb, Trk kinase inhibitors as new treatments for cancer and pain, *Expert Opin Ther Pat*, 19 (2009). 305-319. 10.1517/13543770902721261.

[17] S.E. Skerratt, M. Andrews, S.K. Bagal, J. Bilsland, D. Brown, P.J. Bungay, S. Cole, K.R. Gibson, R. Jones, I. Morao, A. Nedderman, K. Omoto, C. Robinson, T. Ryckmans, K. Skinner, P. Stupple, G. Waldron, The discovery of a potent, selective, and peripherally restricted pan-Trk inhibitor (PF-06273340) for the treatment of pain, *J Med Chem*, 59 (2016). 10084-10099. 10.1021/acs.jmedchem.6b00850.

[18] B. Obermeier, R. Daneman, R.M. Ransohoff, Development, maintenance and disruption of the blood-brain barrier, *Nat Med*, 19 (2013). 1584-1596. 10.1038/nm.3407.

[19] R. Daneman, A. Prat, The blood-brain barrier, *Cold Spring Harb Perspect Biol*, 7 (2015). a020412. 10.1101/cshperspect.a020412.

[20] N. Takayama, N. Sato, S.G. O'Brien, Y. Ikeda, S. Okamoto, Imatinib mesylate has limited activity against the central nervous system involvement of Philadelphia chromosome-positive acute lymphoblastic leukaemia due to poor penetration into cerebrospinal fluid, *Br J Haematol*, 119 (2002). 106-108. 10.1046/j.1365-2141.2002.03881.x.

[21] G. Subramanian, Y. Zhu, S.J. Bowen, N. Roush, J.A. White, D. Huczek, T. Zachary, C. Javens, T. Williams, A. Janssen, A. Gonzales, Lead identification and characterization of hTrkA type 2 inhibitors, *Bioorg Med Chem Lett*, 29 (2019). 126680. 10.1016/j.bmcl.2019.126680.

[22] B. Wang, W. Zhang, X. Liu, F. Zou, J. Wang, Q. Liu, A. Wang, Z. Hu, Y. Chen, S. Qi, Z. Jiang, C. Chen, C. Hu, L. Wang, W. Wang, Q. Liu, J. Liu, Discovery of (E)-N-(4-methyl-5-(3-(2-(pyridin-2-yl)vinyl)-1H-indazol-6-yl)thiazol-2-yl)-2-(4-methylpiperazin-1-yl)acetamide (IHMT-TRK-284) as a novel orally available Type II TRK kinase inhibitor capable of overcoming multiple resistant mutants, *Eur J Med Chem*, (2020). 10.1016/j.ejmech.2020.112744.

[23] S. Cui, Y. Wang, Y. Wang, X. Tang, X. Ren, L. Zhang, Y. Xu, Z. Zhang, Z.M. Zhang, X. Lu, K. Ding, Design, synthesis and biological evaluation of 3-(imidazo[1,2-a]pyrazin-3-ylethynyl)-2-methylbenzamides as potent and selective pan-tropomyosin receptor kinase (TRK) inhibitors, *Eur J Med Chem*, 179 (2019). 470-482. 10.1016/j.ejmech.2019.06.064.

[24] [illegible] Loudon, P. Siebenga, D. Gorman, K. Gore, P. Dua, G. van Amerongen, J.L. Hay, G.J. Groeneveld, R. [illegible] Bu[illegible], Demonstration of an anti-hyperalgesic effect of a novel pan-Trk inhibitor PF-06273340 in a battery of human evoked pain models, *Br J Clin Pharmacol*, 84 (2018). 301-309. 10.1111/bcp.13448.

[25] W. Yan, Z. Huang, Z. Wang, S. Cao, L. Tong, T. Zhang, C. Wang, L. Zhou, J. Ding, C. Luo, J. Zhou, H. Xie, W. Duan, Discovery of 1,3-diaryl-pyridones as potent VEGFR-2 inhibitors: design, synthesis, and biological evaluation, *Chem Biol Drug Des*, 87 (2016). 694-703. 10.1111/cbdd.12703.

[26] W. Yan, X. Wang, Y. Dai, B. Zhao, X. Yang, J. Fan, Y. Gao, F. Meng, Y. Wang, C. Luo, J. Ai, M. Geng, W. Duan, Discovery of 3-(5'-substituted)-benzimidazole-5-(1-(3,5-dichloropyridin-4-yl)ethoxy)-1*H*-indazoles as potent fibroblast growth factor receptor inhibitors: design, synthesis, and biological evaluation, *J Med Chem*, 59 (2016). 6690-6708. 10.1021/acs.jmedchem.6b00056.

[27] B. Frett, F. Carlomagno, M.L. Moccia, A. Brescia, G. Federico, V. De Falco, B. Admire, Z. Chen, W. Qi, M. Santoro, H.Y. Li, Fragment-based discovery of a dual pan-RET/VEGFR2 kinase inhibitor optimized for single-agent polypharmacology, *Angew Chem Int Ed Engl*, 54 (2015). 8717-8721. 10.1002/anie.201501104.

[28] M. Moccia, B. Frett, L. Zhang, N.R. Lakkaniga, D.C. Briggs, R. Chauhan, A. Brescia, G. Federico, W. Yan, M. Santoro, N.Q. McDonald, H.Y. Li, F. Carlomagno, Bioisosteric discovery of NPA101.3, a second-generation RET/VEGFR2 inhibitor optimized for single-agent polypharmacology, *J Med Chem*, 63 (2020). 4506-4516. 10.1021/acs.jmedchem.9b01336.

[29] N.R. Lakkaniga, N. Gunaganti, L. Zhang, B. Belachew, B. Frett, Y.K. Leung, H.Y. Li, Pyrrolo[2,3-d]pyrimidine derivatives as inhibitors of RET: Design, synthesis and biological evaluation, *Eur J Med Chem*, 206 (2020). 112691. 10.1016/j.ejmech.2020.112691.

[30] N.R. Lakkaniga, L. Zhang, B. Belachew, N. Gunaganti, B. Frett, H.Y. Li, Discovery of SP-96, the first non-ATP-competitive Aurora Kinase B inhibitor, for reduced myelosuppression, *Eur J Med Chem*, 203 (2020). 112589. 10.1016/j.ejmech.2020.112589.

[31] B. Frett, N. McConnell, Y.X. Wang, Z.G. Xu, A. Ambrose, H.Y. Li, Identification of pyrazine-based TrkA inhibitors: design, synthesis, evaluation, and computational modeling studies, *Medchemcomm*, 5 (2014). 1507-1514. 10.1039/c4md00251b.

[32] J.L. Woodring, G. Patel, J. Erath, R. Behera, P.J. Lee, S.E. Leed, A. Rodriguez, R.J. Sciotti, K. Mensa-Wilmot, M.P. Pollastri, Evaluation of aromatic 6-substituted thienopyrimidines as scaffolds against parasites that cause trypanosomiasis, leishmaniasis, and malaria, *MedChemComm*, 6 (2015). 339-346. 10.1039/C4MD00441H.

[33] T. Bertrand, M. Kothe, J. Liu, A. Dupuy, A. Rak, P.F. Berne, S. Davis, T. Gladysheva, C. Valtre, J.Y. Crenne, M. M[illegible]hi, The crystal structures of trkA and trkB suggest key regions for achieving selective inhibition, *J Mol Biol*, 423 (2012). 43[illegible]-453. 10.1016/j.jmb.2012.08.002.

[34] D. Saha, A. Kharbanda, W. Yan, N.R. Lakkaniga, B. Frett, H.Y. Li, The Exploration of Chirality for Improved Druggability within the Human Kinome, *J Med Chem*, 63 (2020). 441-469. 10.1021/acs.jmedchem.9b00640.

[35] M. Menichincheri, E. Ardini, P. Magnaghi, N. Avanzi, P. Banfi, R. Bossi, L. Buffa, G. Canevari, L. Ceriani, M. Colombo, L. Corti, D. Donati, M. Fasolini, E. Felder, C. Fiorelli, F. Fiorentini, A. Galvani, A. Isacchi, A.L. Borgia, C. Marchionni, M. Nesi, C. Orrenius, A. Panzeri, E. Pesenti, L. Rusconi, M.B. Saccardo, E. Vanotti, E. Perrone, P. Orsini, Discovery of entrectinib: a new 3-aminoindazole as a potent anaplastic lymphoma kinase (ALK), c-ros oncogene 1 kinase (ROS1), and pan-tropomyosine receptor kinases (Pan-TRKs) inhibitor, *J Med Chem*, 59 (2016). 3392-3408. 10.1021/acs.jmedchem.6b00064.

[36] R. Cecchelli, S. Aday, E. Sevin, C. Almeida, M. Culot, L. Dehouck, C. Coisne, B. Engelhardt, M.P. Dehouck, L. Ferreira, A stable and reproducible human blood-brain barrier model derived from hematopoietic stem cells, *PLoS One*, 9 (2014). e99733. 10.1371/journal.pone.0099733.

[37] D.C. Pedroso, A. Tellechea, L. Moura, I. Fidalgo-Carvalho, J. Duarte, E. Carvalho, L. Ferreira, Improved survival, vascular differentiation and wound healing potential of stem cells co-cultured with endothelial cells, *PLoS One*, 6 (2011). e16114. 10.1371/journal.pone.0016114.

[38] W. Risau, A. Dingler, U. Albrecht, M.P. Dehouck, R. Cecchelli, Blood-brain barrier pericytes are the main source of gamma-glutamyltranspeptidase activity in brain capillaries, *J Neurochem*, 58 (1992). 667-672. 10.1111/j.1471-4159.1992.tb09769.x.

[39] M. Heymans, R. Figueiredo, L. Dehouck, D. Francisco, Y. Sano, F. Shimizu, T. Kanda, R. Bruggmann, B. Engelhardt, P. Winter, F. Gosselet, M. Culot, Contribution of brain pericytes in blood-brain barrier formation and maintenance: a transcriptomic study of cocultured human endothelial cells derived from hematopoietic stem cells, *Fluids Barriers CNS*, 17 (2020). 48. 10.1186/s12987-020-00208-1.

[40] F. Nolay, E. Sevin, M. Leteve, A. Bil, F. Gosselet, K. El Kirat, F. Djedaini-Pilard, S. Morandat, L. Fenart, C. Przybylski, V. Bonnet, First step to the improvement of the blood brain barrier passage of atazanavir encapsulated in sustainable bioorganic vesicles, *Int J Pharm*, 587 (2020). 119604. 10.1016/j.ijpharm.2020.119604.

[41] J. Yerri, J. Dias, M.R. Nimmakayala, F. Razafindrainibe, C. Courageux, A.J. Gastellier, J. Jegoux, C. Coisne, C. Landry, F. Gosselet, J. Hachani, J.F. Goossens, M.P. Dehouck, F. Nachon, R. Baati, Chemoselective Hydrogenation of 6-Alkynyl-3-fluoro-2-pyridinaldoximes: Access to First-in-Class 6-Alkyl-3-Fluoro-2-pyridinaldoxime Scaffolds as New Reactivators of Sarin-Inhibited Human Acetylcholinesterase with Increased Blood-Brain Barrier Permeability, *Chemistry*, 26 (2020). 15035-15044. 10.1002/chem.202002012.

[42] A.G. Calas, A.S. Hanak, N. Jaffre, A. Nervo, J. Dias, C. Rousseau, C. Courageux, X. Brazzolotto, P. Villa, A. Obrecht, J.F. Goossens, C. Landry, J. Hachani, F. Gosselet, M.P. Dehouck, J. Yerri, M. Kliachyna, R. Baati, F. Nachon, Efficacy Assessment of an Uncharged Reactivator of NOP-Inhibited Acetylcholinesterase Based on Tetrahydroacridine Pyridine-Aldoxime Hybrid in Mouse Compared to Pralidoxime, *Biomolecules*, 10 (2020). 10.3390/biom10060858.

[43] M.P. Dehouck, P. Jolliet-Riant, F. Bree, J.C. Fruchart, R. Cecchelli, J.P. Tillement, Drug transfer across the blood-brain barrier: correlation between in vitro and in vivo models, *J Neurochem*, 58 (1992). 1790-1797. 10.1111/j.1471-4159.1992.tb10055.x.

[44] A. Siflinger-Birnboim, P.J. Del Vecchio, J.A. Cooper, F.A. Blumenstock, J.M. Shepard, A.B. Malik, Molecular sieving characteristics of the cultured endothelial monolayer, *J Cell Physiol*, 132 (1987). 111-117. 10.1002/jcp.1041320115.

Graphical abstract:

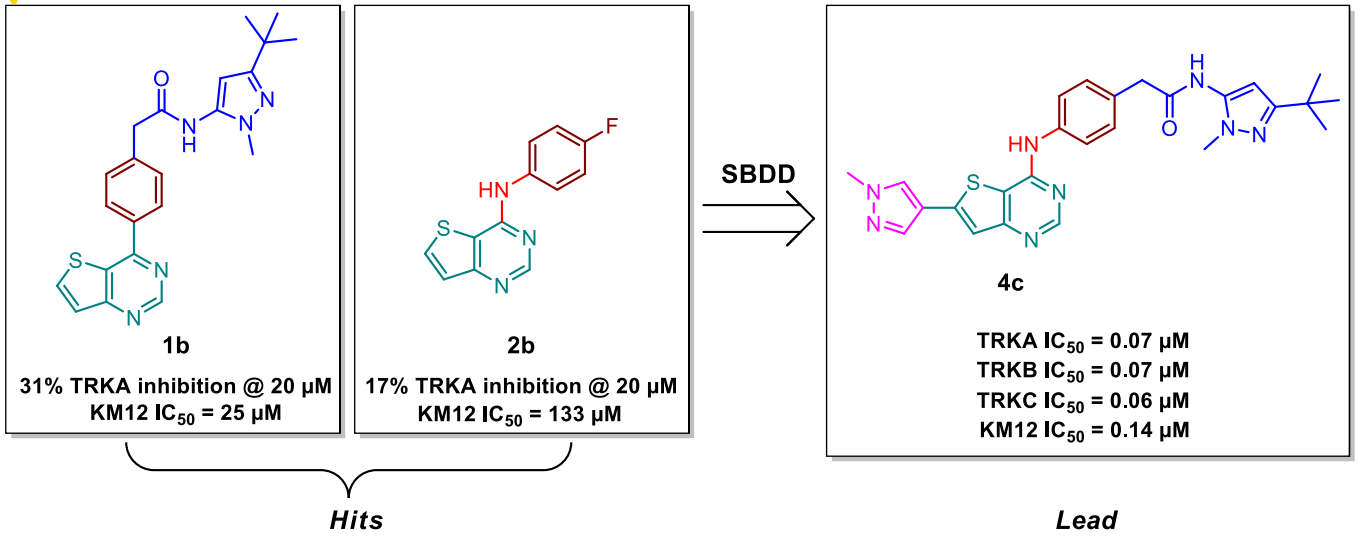

Highlights:

- A series of novel thieno[3,2-*d*]pyrimidine type-II pan-TRK inhibitors were designed and synthesized.
- Representative compound **4c** was discovered through structure-based drug design (SBDD) approach
- Compound **4c** exhibited an effective blockage of TRKA autophosphorylation.
- Compound **4g** exhibited excellent selectivity for KM12 in the NCI-60 human cancer cell lines screen